Reviewed Preprint
v1 • March 24, 2026
Not revised

Reviewed Preprint
v2 • May 8, 2026
Revised by authors

For correspondence:
stephan.gruber@unil.ch

Competing interests: No competing interests declared

Funding: See page 20

Reviewing editor: Adèle L Marston, University of Edinburgh, United Kingdom

Single Domain Antibody Inhibitors Target the Coiled Coil Arms of the *Bacillus subtilis* SMC complex

Ophélie Gosselin[1], Michael Taschner[1], Lea M Huber-Hürlimann[2], Markus A Seeger[2], Stephan Gruber[1]

[1]Department of Fundamental Microbiology (DMF), Faculty of Biology and Medicine (FBM), University of Lausanne (UNIL), Lausanne, Switzerland • [2]Institute of Medical Microbiology, University of Zurich, Zürich, Switzerland

eLife Assessment

This **important** study introduces an innovative synthetic nanobody approach to probe the function of the bacterial SMC complex. The work is a **compelling** example of the potential of this approach. The authors generate protein chimeras to provide **convincing** evidence that their identified nanobodies target the coiled-coil region of the SMC subunit, demonstrating that this region is critical for SMC function in vivo. Overall, the work is significant for the fields of genome organisation, SMC protein biology, synthetic biology, and bacterial cell biology.

[Editors' note: this paper was reviewed by *Review Commons*.]

https://doi.org/10.7554/eLife.111131.2.sa4

Abstract

Synthetic nanobodies—also called sybodies—have proven valuable for stabilizing conformations of purified proteins, advancing structural and functional studies for example of transmembrane protein complexes. However, their utility in modulating protein function in living cells has remained less well explored. Structural Maintenance of Chromosomes (SMC) complexes facilitate chromosome organization by DNA loop extrusion, a fundamental process in all domains of life. In this study, we target the bacterial SMC complex, Smc-ScpAB, in *Bacillus subtilis* with synthetic nanobodies, aiming to identify key functional regions of the protein complex in a largely unbiased manner. We first isolate sybodies that specifically bind purified Smc-ScpAB and then express them in *B. subtilis* to select binders capable of disrupting Smc-ScpAB function, leading to chromosome segregation defects and cell death. Mapping and biochemical characterization show that the fourteen disruptive sybodies belong to one of three library designs, target the Smc subunit near the same coiled coil arm interface and modulate its ATPase activity in two principal ways, highlighting the mid-region of the Smc coiled coil as critical feature of the DNA folding process. These findings underscore the potential of sybodies—and, by extension, designed binders—as versatile tools for probing dynamic protein function in living cells, with potentially broad applications in cell and synthetic biology.

Introduction

Rapid and specific interference with protein activity and dynamics in living cells is essential for studying and understanding biological mechanisms. However, current approaches—primarily based on small-molecule inhibitors—remain laborious, time-consuming, and costly. The advent of conformation-specific synthetic nanobody (sybody) selection [1], and more recently, computational design of protein binders [2], offer unique opportunities for protein-based inhibition and modulation of cellular targets. Here, we generate sybodies against the SMC complex in *B. subtilis* to efficiently inhibit its function within cells.

Structural Maintenance of Chromosomes (SMC) complexes are multi-subunit, ring-shaped ATP-hydrolyzing DNA motors that structure chromosomal DNA by loop extrusion. They are essential for chromosome organization and segregation, gene expression, DNA repair, and defense against non-self DNA across all domains of life [3]. Each SMC protein (Smc in *B. subtilis, bsu*Smc) is a long polypeptide with its N- and C-termini folding together to form a globular ATP binding cassette (ABC) "head" domain. The head is connected to a "hinge" dimerization domain via a ~50 nm antiparallel coiled coil "arm", creating an elongated dimer (Figure 1Aii and 1Aiii). ATP binding promotes head engagement, bringing the heads together to form a functional ATPase. Non-SMC subunits, a kleisin (ScpA in *B. subtilis*) and a dimer of KITE (ScpB in *B. subtilis*) or two HAWK proteins, bridge the heads, together forming a ring around DNA (Figure 1Aiii). In *B. subtilis*, Smc-ScpAB is recruited to the origin of replication (*oriC*) region on the chromosome by ParB, a DNA-binding protein that recognizes centromere-like *parS* sequences (Figure 2Ai). Once loaded, Smc-ScpAB translocates at a rate of ~1 kb/s onto flanking DNA, aligning the two chromosome arms and individualizing nascent sister chromosomes[4–6], likely bypassing obstacles on the chromosome through the SMC hinge gate [7]. Null mutants of *smc*, *scpA*, or *scpB* fail to segregate chromosomes properly and lose viability under conditions promoting rapid growth[5,6,8].

Several models have been proposed for the mechanism of DNA loop extrusion by SMC complexes, including the "segment capture" model, in which DNA segments are transiently trapped between the SMC arms in partially open states and fused into larger loops through iterative ATP-driven cycles (Figure 1Aiii and S1B) [9–11]. However, detailed structural understanding and experimental testing *in vivo* are lacking.

Antibodies can block biochemical reactions by stabilizing reaction intermediates. Synthetic single-domain antibodies called sybodies are small, robust antigen-binding proteins that were engineered based on three camelid nanobody structures [1]. They are selected from synthetic libraries that encode a wide diversity of binding surfaces and epitope shapes based on the length and geometry of their CDR3 loop, allowing strong binding of diverse antigen surfaces (Figure 1Ai). Their small size (~15 kDa), stability, and ability to bind transient epitopes make them ideal tools for targeting specific states of biomolecules [12]. Selection is carried out using purified and immobilized Smc-ScpAB by ribosome display and phage display, typically followed by an ELISA-based screening [1].

Here, we demonstrate that sybodies can be used to interfere with the function of *B. subtilis* Smc-ScpAB *in vivo*. We first isolate binders that specifically target purified Smc-ScpAB *in vitro* and then select those that eliminate Smc function when expressed in *B. subtilis*. Fourteen sybodies were found to disrupt chromosome segregation, mimicking *smc* deletion phenotypes. Biochemical assays confirmed that selected sybodies alter the ATP hydrolysis rate of Smc-ScpAB and its stimulation by DNA addition, likely stabilizing intermediates of the conformational cycle. Mapping experiments using chimeric Smc constructs revealed that most binders, unexpectedly, target the coiled coil, specifically in a defined region near the Smc 4N arm-to-arm contact [13], highlighting the potential of sybodies and designed binders, as genetic tools to identify essential functional domains and underscoring the importance of coiled coil dynamics for Smc function.

Results

Generation of *bsu*Smc-ScpAB-specific sybodies

To isolate sybodies that impede the function of *B. subtilis* Smc-ScpAB complex, we first performed *in vitro* selection with purified Smc-ScpAB in the presence of 40 bp duplex DNA, and an ATPase-deficient mutant (E1118Q) of *bsu*Smc. These conditions favour ATP-engaged complexes alongside the typically predominant ATP-disengaged rod-shaped state [13]. *bsu*Smc was also biotinylated at the hinge at residue R643C for immobilization (Figure 1Aii-iii and S1A) [1,14–16]. Starting from three synthetic sybody libraries encoding distinct epitope-binding geometries (denoted as concave, loop, convex, respectively, Figure 1Ai), we performed one round of ribosome display starting from a large sybody library followed by two rounds of phage display, thereby enriching sybodies that bind to Smc-ScpAB (Table 1). From each library, 95 sybody-expressing *E. coli* clones were

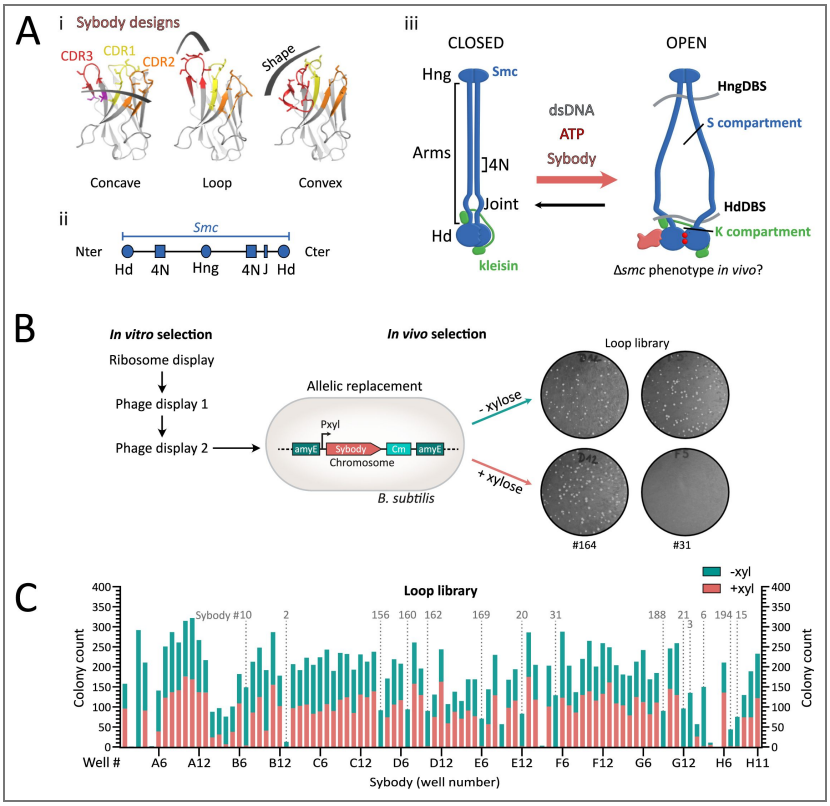

Figure 1. Selection of sybodies targeting *S*mc-ScpAB in *B. subtilis*.

(A) (i) Structural design and randomization scheme of the three synthetic sybody libraries: concave, loop, and convex. Complementarity-determining regions (CDRs) 1, 2, and 3 are shown in yellow, orange, and red, respectively; randomized residues are shown as sticks. Adapted from [1]. **(ii)** SMC domain organization. The N- and C-terminal regions encode half an ATPase head, while the middle domain constitutes the hinge dimerization domain. The elongated sequence in-between encodes for long helical sequences that will form an antiparallel intramolecular coiled coil. Hd: head, Hng: hinge, 4N: 4N arm-to-arm contact, J: joint. **(iii)** SMC complexes harbor juxtaposed arms in their resting state. Upon ATP binding at the heads, the heads dimerize (head engagement), leading to a conformational change of the entire complex in which the arms open. This state is thought to fit a loop of DNA (not shown) in the S compartment formed by the SMC arms, that will be pushed towards the K compartment formed by the heads and kleisin, after ADP release. We hypothesized that SMC-blocking sybodies can stabilize distinct conformation of the *bsuS*mc-ScpAB complex promoted by ATP hydrolysis and DNA binding, potentially inducing a *Δsmc*-like phenotype *in vivo* and enabling biochemical characterization of trapped conformations *in vitro*. Blue: SMC dimer, Green: kleisin ScpA. The ScpB KITE subunits are not represented for the sake of simplicity. HngDBS: Hinge DNA-binding site, HdDBS: Head DNA-binding site. **(B)** Framework for sybody selection. *In vitro* selection starts with ~10^{12} sybody variants per library subjected to ribosome display for pre-enrichment, followed by two rounds of phage display. For *in vivo* selection, 95 randomly selected sybody genes were integrated into the *B. subtilis* chromosome under the control of a xylose-inducible promoter by allelic replacement at the *amyE* locus. Growth defects on rich medium were tested on ONA agar plates with or without 0.5% xylose. Example shown: Sb164 (loop library) did not affect growth, whereas Nb31 impaired growth upon induction, suggesting interference with *bsuS*mc function. **(C)** Growth assay results for the 95 *B. subtilis* strains expressing individual xylose-inducible sybodies of the loop library. Bars show colony counts “without” (green) on top of “with” (pink) xylose. Strains are ordered by their original position in the 96-well plate. Fourteen sybodies consistently impaired colony formation under inducing conditions (marked by dotted lines). Sybody numbers indicated above the plots correspond to selected candidates used in subsequent experiments, numbering according to order of first use. Notably, the strain corresponding to the E09 sybody (Sb018), showed an absence of colonies upon sybody induction. However, this sybody candidate gave intermediate phenotypes in later experiments, which is why it was excluded from detailed analysis.

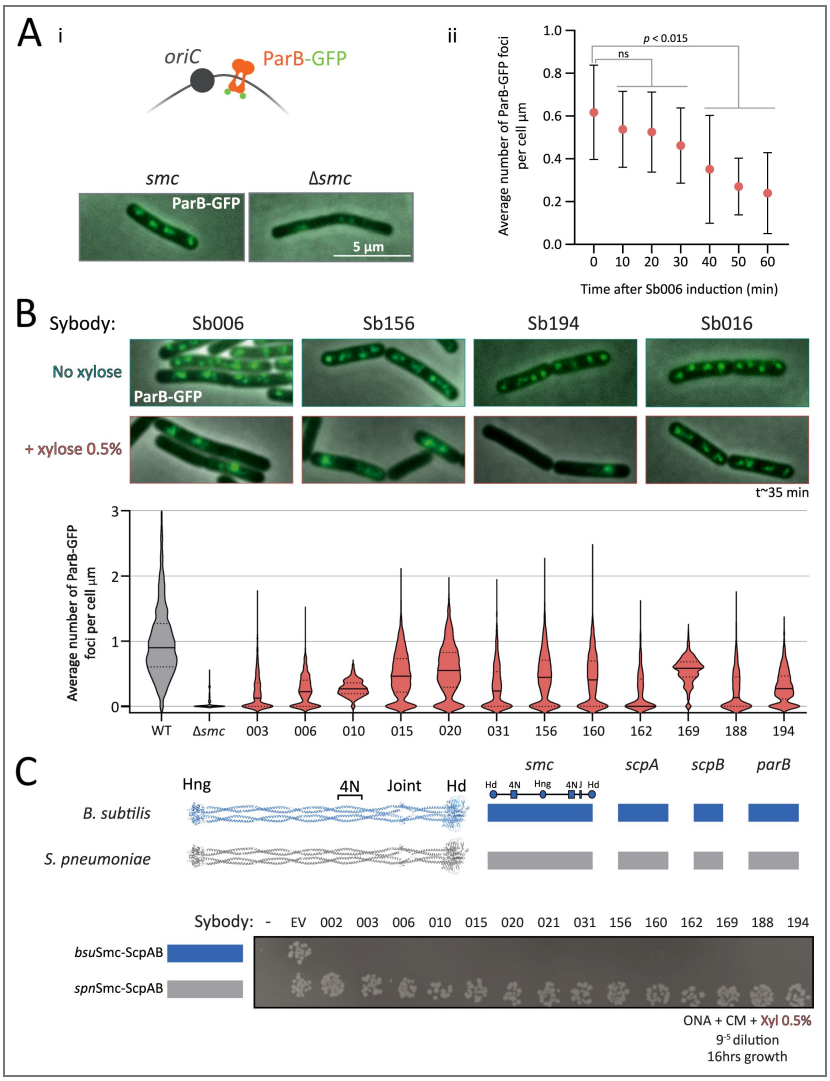

Figure 2. Sybody-induced chromosome segregation defects visualized by ParB-GFP imaging.

(A) i, *Top*: Schematic illustrating ParB-GFP binding near *oriC*, enabling visualization of origin positioning. *Bottom*: Representative images showing ParB-GFP foci in wild-type and *Δsmc B. subtilis*. *Smc* WT cells typically display 2–4 foci per cell, whereas *Δsmc* cells exhibit reduced foci numbers. ii, Number of ParB-GFP foci per µm of cell length in a strain carrying inducible sybody Sb006. A significant decrease in foci is detected from 40 minutes post-induction (p_{t0-10} = 0.9674; p_{t0-20} = 0.9033; p_{t0-30} = 0.3744; p_{t0-40} = 0.0145; p_{t0-50} = 0.0004; p_{t0-60} < 0.001). Based on this, a standardized induction time of ~35 minutes was used in subsequent experiments. **(B)** ParB-GFP foci density (foci/µm) in WT, *Δsmc,* and sybody-expressing strains after 35 minutes of xylose induction. Violin plots show distribution per condition; solid lines denote the mean, and dotted lines indicate quartiles. Several hundreds of cells were analyzed (between 351 and 1735), except for *Δsmc* and Sb010 were fewer cells were available (134 and 73, respectively). **(C)** Spot assay to assess colony formation of *B. subtilis* strains *bsu* or *spn* variants of Smc-ScpAB and ParB. *Top*: Schematic shows gene origins (blue: *B. subtilis*; grey: *S. pneumoniae*). The leftmost column corresponds to the parental *B. subtilis* strain 1A700 carrying the *S. pneumoniae* genes without chloramphenicol resistance (non-growing). The next spots represent the same strains carrying no sybody gene but the Cm resistance (EV for empty vector). Remaining spots are sybody-expressing strains; sybody numbers are indicated above. Cells were grown for 16 h at 37 °C on ONA supplemented with 0.5% xylose and chloramphenicol. Hd: head, Hng: hinge, 4N: 4N arm-to-arm contact, J: joint.

randomly chosen for *in vivo* characterization. ELISA data revealed that nearly all clones bind purified Smc-ScpAB (Table 1). However, the ELISA signals of only few Sybodies showed clear dependence on the presence or absence of ATP and DNA (Table S1).

Identification of *bsu*Smc-ScpAB-blocking sybodies through phenotypic screening in *B. subtilis*

We therefore decided to screen for inhibiting sybodies directly in *B. subtilis* cells. Despite containing a conserved disulfide bond, sybodies have been successfully expressed inside cells and were shown to bind their targets in the reducing environment of the cytoplasm, likely owing to their robust folding [17]. To assess whether the selected sybodies interfere with Smc function *in vivo*, each of the 285 sybody sequences was cloned under a xylose-inducible promoter (P_{xyl}) into an *E. coli–B. subtilis* shuttle vector and integrated at the *amyE* locus of the wild-type 1A700 strain (Figure 1B) [18]. Fourteen sybodies from the loop library failed to yield transformants in the presence (but not absence) of xylose, indicating cell lethality due to sybody inhibition of Smc-ScpAB (Figure 1C, S2A-B). These Smc-disruptive sybodies (denoted as Sb002, 003, 006, 010, 015, 020, 021, 031, 156, 160, 162, 169, 188, and 194, respectively) harbor fourteen distinct sequences(Table S2). Intriguingly, no such disruptive sybodies were isolated from the concave and convex libraries (Figure S2B), suggesting that the CDR3 geometry as present in the loop library is particularly effective at inhibiting *bsu*Smc-ScpAB. Likely, sybodies of the other libraries bound to other epitopes of *bsu*Smc-ScpAB that are not sensitive to conformational trapping, and it is further possible that they were not stably expressed in *B. subtilis*. However, at least for sybodies from the loop library, we did not notice any obvious correlation between expression levels and phenotypes. Selected sybodies showed similar expression and were appreciably expressed even without inducer (Figure S4, S5). Notably, tendencies of preferential isolation of binders from one of the three libraries have previously been observed, although at milder levels [1,17,19].

Selected sybodies target *bsu*Smc-ScpAB function *in vivo*

To determine whether the fourteen sybodies indeed impair chromosome segregation, we used fluorescence microscopy to monitor *oriC* positioning in a *B. subtilis* strain expressing a ParB-GFP fusion protein together with a P_{xyl}-inducible sybody gene. In these strains, ParB-GFP marks the replication origin region by binding to *parS* sites near *oriC* (Figure 2Ai). As expected, the *Δsmc* strain displayed fewer ParB-GFP foci and elongated cells (Figure 2Ai) (Table S3). These elongated cells are known to harbour expanded nucleoids, consistent with delayed *oriC* separation rather than delayed DNA replication [6,20]. A time course experiment using sybody Sb006 revealed chromosome organization defects as early as 30 minutes post induction, with a significant reduction in ParB-GFP foci per μm cell length at 40 minutes (p = 0.0145) (Figure 2Aii). Subsequent imaging was performed ~35 minutes after induction of sybody expression.

All disruptive sybodies reduced ParB-GFP foci density compared to the control (1.03 foci/μm), with values ranging from 0.56 foci/μm (Sb020) to 0.22 foci/μm (Sb003). These defects were all robustly detected, while being less severe than the Δ*smc* mutant (~0.05 foci/μm), conceivably due to the short induction time or incomplete inhibition. Milder defects were also observed without induction, likely attributed to leaky expression from the P_{xyl} promoter (Figure S3A). Sybody expression also caused cell elongation and growth delays, both hallmarks of impaired Smc activity, consistent with chromosome segregation defects that delay cell division (Figure S3B–C). Altogether, these results show that all selected sybodies induce *Δsmc*-like phenotypes likely by interfering with *bsu*Smc-ScpAB activity *in vivo*.

Selected sybodies specifically target *B. subtilis* Smc-ScpAB

To test whether sybodies specifically target *B. subtilis* Smc-ScpAB, we assessed their effects in a strain expressing *Streptococcus pneumoniae* (*Spn*) Smc-ScpAB and ParB proteins in place of the endogenous *B. subtilis* proteins. The *Spn* sequences can functionally replace the corresponding *Bsu* sequences despite significant sequence divergence (~38% sequence identity) [21]. Strikingly, none of the sybodies impaired growth in this background, even though a cognate ParAB pair is absent in

	Ribosome Display (qPCR)		Phage Display (qPCR)	
Library	**Total #of RNAs**	**Titer (PFU/mL)**	**Enrichment 1**	**Enrichment 2**
Convex (S)	1.36×10^{8}	8.96×10^{13}	3.1×	1474.7×
Loop (M)	6.95×10^{7}	5.46×10^{13}	1.4×	1209.9×
Concave (L)	1.25×10^{8}	8.32×10^{13}	1.8×	1808.0×

Table 1. Sybody enrichments at different steps of the selection procedure.

Ribosome display output was quantified by qPCR, while phage display results include final phage titers and enrichment values from rounds one and two, also measured by qPCR.

this strain (*S. pneumoniae* lacks *parA*), sensitizing cells to chromosome segregation defects (Figure 2C). These results confirm that the sybodies are specific to *bsu*Smc-ScpAB and that off-target toxicity is not noticeable.

*bsu*Smc-ScpAB-disrupting sybodies target two distinct coiled coil regions adjacent to the *bsu*Smc 4N arm-to-arm contact

To map the sybody-binding site on the *bsu*Smc-ScpAB complex, we utilized five chimeric Smc constructs (Smc Chimera 1-5), in which the hinge and progressively longer segments of the adjacent coiled coils were replaced with the corresponding sequences from the *S. pneumoniae* Smc protein (Figure 3A). Chimeric junctions were designed to preserve coiled coil integrity based on available crystal structures, coiled coil predictions by DeepCoil, and AlphaFold2 structural models [1,22,23]. All chimeric Smc strains retained the native *B. subtilis scpA*, *scpB*, and *parB* genes and were viable under conditions promoting fast growth, demonstrating proper protein folding and functioning of chimeric Smc-ScpAB complexes (Figure S6A).

Chimeras 1 and 2, which carry the central hinge and coiled coil sequences of *Spn* origin (residues 363-812 and 339-836, respectively), showed the same sybody-induced growth defects as the wild-type strain, indicating that the sybodies bind further away from the hinge, within the remaining *B. subtilis* portion comprising of the Smc head and the first ~230 coiled coil residues, and ScpAB (Figure 3A). By contrast, Chimera 5 (residues 248–927 of *Spn* origin), supported robust growth even in the presence of the *bsu*Smc-disrupting sybodies, indicating that the region comprising the heads and first ~50 residues of the coiled coil (including the joint) does not comprise the binding site. The binding region for the sybodies is thus located on the coiled coil between residues 248 and 339 (or 836 and 927), demonstrating that all fourteen sybodies bind to a central region of the coiled coil.

Chimera 3 (*spn*Smc residues 318-857) and chimera 4 (*spn*Smc residues 276-899) revealed two distinct sybody responses. Sb003, 031, 156, 160, 162, and 169 impaired growth of both strains, mapping their binding sites to *B. subtilis* residues 248-276 (and 899-927), present in chimeras 1–4 but absent in chimera 5. In contrast, Sb002, 006, 010, 015, 020, 021, 188, and 194 had no impact on the viability of chimera 3 or 4, suggesting they target residues 318-339/836-857 (Figure 3A, 3D).

In sum, these experiments mapped the binding sites of all fourteen disruptive sybodies to one of two ~twenty amino acid segments in the central region of the *bsu*Smc coiled coil (Figure 3D). These regions harbor relatively poorly conserved sequences but flank the 4N arm-arm contact (~at residue 295), previously proposed to serve as an essential structural switch between closed and open conformations[13]. These results reveal that all isolated sybodies target the same functional element of the Smc arms, and that interfering with this element disrupts Smc-dependent chromosome organization *in vivo*.

Smc-disrupting sybodies affect the ATPase activity in one of two ways

To investigate how sybodies may influence *bsu*Smc-ScpAB, we next measured ATP hydrolysis rates using purified proteins in the presence and absence of DNA. SMC ATPase activity serves as an indirect readout for state transitions, including arm opening and head engagement. In absence of DNA, *bsu*Smc-ScpAB hydrolyzes ATP at ~4 ATP/min/Smc [13]. DNA binding stimulates ATP hydrolysis to ~9 ATP/min/Smc, presumably by DNA binding promoting arm opening and head engagement, creating a more open conformation.

All disruptive sybodies measurably affected the ATP hydrolysis rate of *bsu*Smc-ScpAB. Ten maintained a near-basal ATPase rate even in presence of DNA (Sb002, Sb003, Sb010, Sb031, Sb156, Sb160, Sb162, Sb169, Sb188, and Sb194) (Figure 3B-C and S6B). This suggests that they stabilize the complex in a closed or partially closed conformation, thus hindering DNA-dependent ATPase stimulation. Notably, in this group, Sb002 and Sb194 showed slightly elevated ATPase rates with DNA, hinting at a mildly more flexible conformation.

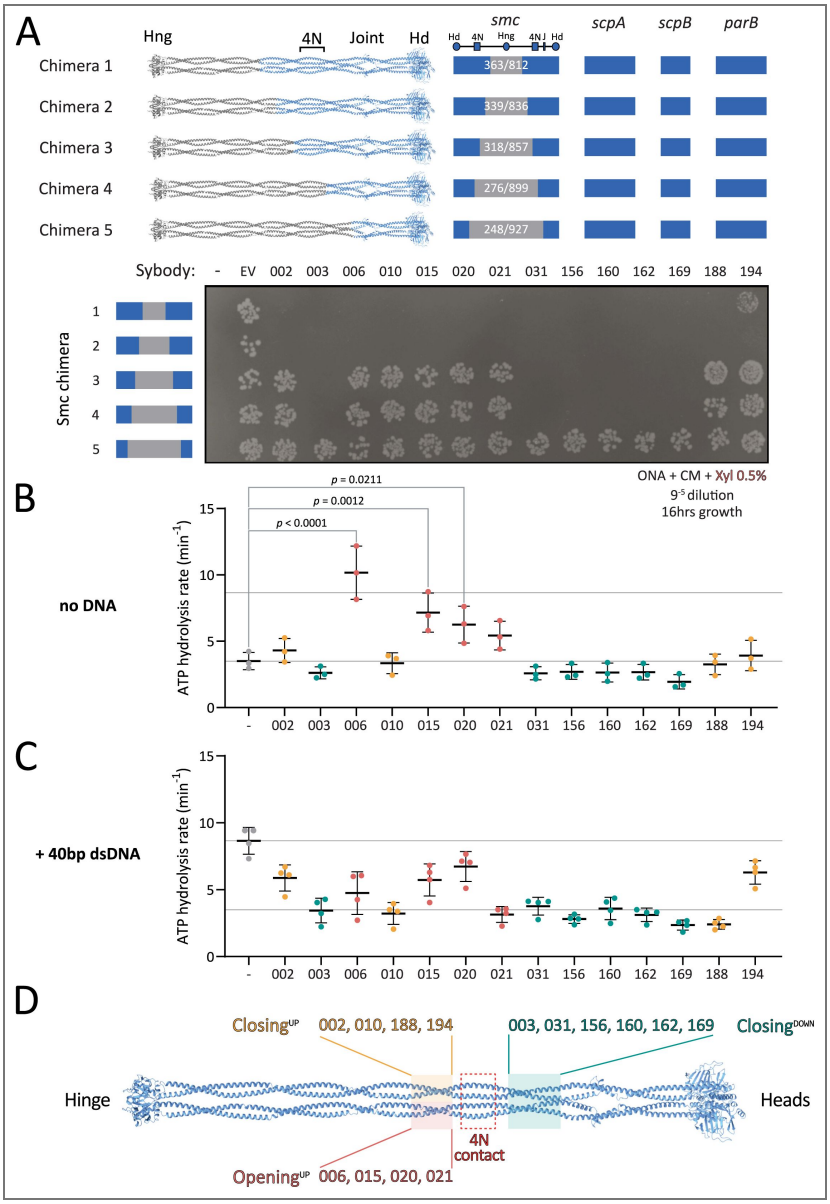

Figure 3. Mapping sybody binding sites on Smc-ScpAB.

(A) Colony formation of *B. subtilis* strains expressing chimeric Smc-ScpAB complexes comprising *S. pneumoniae* and *B. subtilis* sequences. The schematic above the spot assay depicts the species origin of the *smc* gene, the *scpAB* operon and *parB* gene (blue: *B. subtilis*; grey: *S. pneumoniae*). "–" indicates no insertion at the *amyE* locus; "EV" refers to the empty vector control containing only the chloramphenicol resistance cassette that was inserted in *amyE*; numbered labels correspond to sybodies. Cells were spotted on rich medium (ONA) supplemented with chloramphenicol and xylose and incubated for 16 h at 37 °C. Hd: head, Hng: hinge, 4N: 4N arm-to-arm contact, J: joint. **(B)** ATP hydrolysis rates of *bsu*Smc-ScpAB in the presence of sybodies but absence of DNA. Significant effects by one-way ANOVA are indicated by p values. **(C)** ATPase rates in the presence of 40 bp dsDNA. All sybodies significantly reduced DNA-stimulated ATP hydrolysis. Reported p-values: Sb020 (p = 0.340), Sb194 (p = 0.0049), Sb002 (p = 0.0007), Sb015 (p = 0.0003); all others, p < 0.0001. **(D)** Schematic summary of sybody binding sites mapped onto the Smc dimer, categorized by their effect on ATPase activity. Sybodies are grouped based on functional impact and mapped to corresponding structural regions: pink/yellow boxes indicate residues 318–339 and 836–857; green boxes mark residues 248–276 and 899–927; and the red box highlights the 4N contact region (approx. residues 290–320).

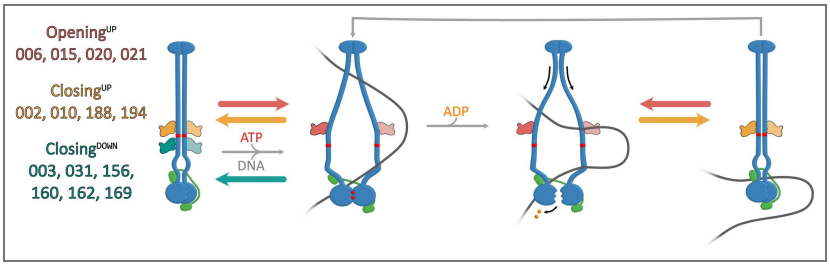

Figure 4. Proposed models for sybody interactions with *bsu*Smc-ScpAB during the ATPase cycle.

(A) Model for sybodies of the Opening^{UP}, Closing^{UP} and Closing^{DOWN} group. Opening^{UP} sybodies, likely prevent complete arm closure. In the presence of DNA, these sybodies may stabilize a suboptimal conformation for head disengagement, resulting in reduced ATPase activity (not shown here). Closing^{UP} and Closing^{DOWN} sybodies stabilize a closed-arm conformation. These likely hinder DNA segments from entering the inter-arm space and accessing the hinge-proximal DNA binding site.

In contrast, the other sybodies (Sb006, Sb015, Sb020, and Sb021) stimulated ATP hydrolysis in the absence of DNA, with Sb006 reaching levels comparable to DNA-induced activation (~10 ATP/min). This implies that these sybodies stabilize Smc-ScpAB in a more open state promoting head engagement. Curiously, addition of DNA in the presence of Sb006 and Sb021 reduced—rather than stimulated—ATPase activity (Figure 3B-C), suggesting that concurrent DNA and sybody binding may trap the complex in a non-productive conformation, perhaps by favoring the open state excessively. These findings are consistent with the idea that 4N contact region plays a critical role in arm opening and ATPase stimulation.

Interestingly, the observed ATPase profiles correlate with distinct binding regions along the Smc arms. All ATPase-stimulating sybodies (Sb006, Sb015, Sb020, Sb021) bind above the 4N contact ("Opening^{UP}"), while sybodies that hinder DNA stimulation fall into two subgroups: those binding above the 4N contact (Sb002, Sb010, Sb188, Sb194—"Closing^{UP}") and those binding below it (Sb003, Sb031, Sb156, Sb160, Sb162, Sb169—"Closing^{DOWN}") (Figure 3D). These results indicate that the sybodies perturb *bsu*Smc-ScpAB in two principal ways: either by favoring the opening of the arms or by constraining the arms in a more closed state. The results highlight arm opening and closure as central regulatory features of bacterial Smc-ScpAB [9,11,24,25] and confirm the key role of the 4N arm contact in balancing the opening and closing of SMC arms [13].

Discussion

Over the past three decades, nanobodies and their synthetic counterparts have transformed biomedical research and structural biology by enabling the targeting and stabilization of transient protein conformations. Despite these advances, their application to probing protein function in living cells has remained limited [17,26]. Here, we expand the utility of sybody selection by employing it as a tool to screen for genetic probes targeting the function of selected molecular machines *in vivo*. This strategy combines the advantages of controlled biochemical reconstitution with the ability to study the function of proteins in their native context. Importantly, sybody selection requires no prior knowledge of vulnerable regions, providing an unbiased means to interrogate protein function that is difficult to achieve through rational design. Our study based on the *B. subtilis* Smc-ScpAB DNA motor as a model uncovers a central regulatory region in the coiled coil arms of Smc and highlight how distinct arm conformations shape SMC function in loop extrusion and chromosome segregation.

Revealing Smc arm dynamics through synthetic binders

All fourteen Smc-disrupting sybodies share the loop library design. Moreover, their Smc binding sites map to the two short coiled coil segments flanking the conserved 4N arm-to-arm contact, a region that has previously been implicated in key conformational transitions during arm opening [13]. While the fourteen sybodies harbour different epitope binding sequences, we suspect that they may all bind to the Smc dimer in an analogous manner. With the long CDR3 loops known to bind narrow structural cavities[12,27], we speculate that these sybodies may intercalate between the two coiled coil arms (Figure 3D). Structural studies are needed to test this hypothesis directly, however, our attempts at X-ray crystallography and electron microscopy of Smc-sybody complexes have failed so far.

Notably, while the coiled coil dimer appears similarly structured from the elbow to the hinge [9] (Figure 3D), no Smc-disrupting sybodies mapped to regions further away from the 4N contact (Figure 3D). This indicates that opening and closure of the Smc arms might be dispensable at these places, although formal testing would require isolating binders efficiently targeting these regions, potentially facilitated by binder design, and expressing them in *B. subtilis*. This parallels with recent findings with the bacterial SMC defense system Wadjet, where hinge-proximal arm opening is dispensable for loop extrusion, but essential for obstacle bypass [7]. Alternatively, these arm-to-arm contacts might be more stable and thus less likely to be interfered with by sybody binding. Similarly, sybodies targeting below the 4N contact all reduce the ATPase rate (or rather its DNA stimulation), indicating that artificial opening at this position may not disrupt Smc function

(Figure S7). Again, these hypotheses need to be tested more directly. We envision that the design of protein binders may allow us to confirm these observations and further dissect the underlying mechanisms.

This work establishes sybodies as precision tools for blocking ATP-driven machines inside bacterial cells. By targeting allosteric control points in Smc, they enable mechanistic dissection of loop extrusion and open new avenues for studying dynamic complexes *in vivo*. More broadly, the study demonstrates how synthetic binders can trap or block conformations of active chromatin-associated machines, providing a powerful means to probe their mechanisms in living cells. Looking ahead, the rational design of protein binders with tailored geometry and allosteric potential could allow researchers to manipulate and visualize specific conformational states with even greater control and refinement, across both prokaryotic and eukaryotic organisms, while the generation and *in vivo* screening of sybodies remains an attractive approach to gain unexpected biological insights in an unbiased manner.

Material and Methods

Bacillus subtilis strains construction and growth

B. subtilis strains used in this study were derived from the parental strain 1A700. Allelic replacement was achieved via double-crossover recombination at the endogenous *smc* locus using the natural competence method described by [18,28]. Chromosome-integration of sybody genes were performed by transforming a vector containing an *amyE* homologous regions on each side of the recombinant gene of interest, as described in [18]. Transformants were selected on ONA solid medium containing the appropriate antibiotics. Following transformation, strains were purified by single colony isolation and verified through a combination of marker testing, phenotype assessment, PCR, and Sanger sequencing of the *smc* locus, when appropriate. For spot assays, cells were cultured to stationary phase in liquid LB medium, and 9^{-2} and 9^{-5} dilutions were then spotted onto solid ONA medium with chloramphenicol (5 ug/mL) and xylose (0.5% w/v) when induction of the P_{xyl} promoter was required. The strains, plasmids, and oligonucleotides used in this study are listed in Table S4, Table S5 and Table S6, respectively.

For viability assessment, 200 LB medium was inoculated with a 1:1000 dilution of a dense *B. subtilis* culture and grown to stationary phase. The culture was then serially diluted in LB medium. From each dilution (9^{-1} to 9^{-8}), 5 µL was spotted onto LB agar plates containing the appropriate antibiotic selection. Plates were incubated, and viability was assessed by imaging the spots at 16- and 24-hours post-incubation.

Sybody selection

Sybody selection was performed following the protocol by [16], with modifications to include binders specific for the ATP/DNA-stabilized “open” form of the *bsu*Smc-ScpAB complex.

Ribosome Display

The standard WTB buffer (50 mM Tris/acetate pH7.4, 150 mM NaCl, 50 mM MgAc2) and its derivatives were adjusted to 50 mM NaCl to facilitate *bsu*Smc-ScpAB binding to dsDNA. The target complex was assembled by mixing 500 nM *bsu*Smc(C119S, C437S, C826S, E1118Q, R643C)-ScpAB, 2 mM ATP, and 5 µM 40 bp dsDNA in WTB-D-BSA buffer (WTB including 0.5% (w/v) BSA and 0.1% Tween-20), incubated for 15 min at room temperature (RT). The ribosome display panning solution was supplemented with 2 mM ATP and 5 µM dsDNA to maintain binding conditions. Solution panning and biotinylated target capture were conducted at RT to optimize selection for the “open” complex. Washing steps incorporated 2 mM ATP and 5 µm 40 bp dsDNA, while elution, reverse transcription, and cDNA amplification followed the original protocol. Reverse transcribed RNA molecules were quantified by qPCR.

First round of phage display

Phagemid libraries were cloned and electroporated into *E. coli* SS320 as previously described[16]. Phage production was performed using M13KO7 helper phage. The phage display buffer (TBSM) consisted of 20 mM Tris-HCl (pH 7.4), 50 mM NaCl, and 2 mM MgCl2. Target preparation involved incubating 500 nM biotinylated *bsu*Smc(C119S, C437S, C826S, E1118Q, R643C)ScpAB with 2 mM ATP and 5 µM dsDNA in TBSM-BSA-D (TBSM including 0.5% (w/v) BSA and 0.05% Tween-20). Phages (10^{12}/ml) were incubated with the target at 50 nM for 20 min at RT before immobilization on neutravidin-coated plates. Washing (with added 2 mM ATP and 5 µm 40 bp dsDNA) and elution otherwise followed the original protocol, with enrichment assessed by qPCR. Amplified phages were used for a second selection round.

Second round of phage display

Purified phages from the first round were used at 5×10^{13} phages/ml, and the target was prepared as in the first round. Phage-target binding occurred at 50 nM in the presence of ATP and dsDNA, followed by capture on magnetic beads. A competition step using non-biotinylated *bsu*Smc-ScpAB (1 µM) was included before washes with TBSM-D. Phages were eluted and enrichment was determined by qPCR. Phagemids were purified, sub-cloned into the pNb_init vector, and transformed into *E. coli* MC1061.

Growth curve analyses

Growth curves were generated from *B. subtilis* strains grown overnight to exponential phase in LB medium supplemented with 0.5% glucose, incubated at 30°C with shaking. The following day, fresh 5 mL LB cultures were inoculated with the overnight culture to an OD of 0.005 and incubated at 37°C with shaking until reaching an optical density (OD) of 0.05. Subsequently, each culture was subjected to a twofold dilution in a 96-well plate (Costar #3596), achieving a final volume of 200 µL per well. Where necessary, cultures were induced with 0.5% xylose. Plates were incubated at 37°C with continuous shaking in a Thermo Scientific Multiskan FC plate reader. Growth curves were determined by light scattering at 620 nm. The BactEXTRACT app was used to perform Analysis and visualization of the data [29].

Protein purification

Purification of *bsu*Smc and biotinylated *bsu*Smc(C119S, C437S, C826S, E1118Q, R643C)

*bsu*Smc proteins were purified according to [14]. pET-22 or pET-28 plasmids encoding the *Smc* recombinant sequences were transformed into *E. coli* BL21-Gold (DE3) cells. Protein expression was carried out in ZYM-5052 autoinduction medium for 23 hours at 24°C. The cells were harvested and resuspended in lysis buffer (50 mM Tris-HCl, pH 7.5, 150 mM NaCl, 1 mM EDTA, 1 mM DTT, 10% (w/v) sucrose) supplemented with protease inhibitor cocktail. Cell lysis was achieved by sonication, and the lysate was clarified by centrifugation. The supernatant was filtered through a 0.45 µm membrane and loaded onto two HiTrap Blue HP 5 mL columns connected in series. Elution was performed using lysis buffer with 1 M NaCl. The main peak fractions were pooled and diluted with salt-free buffer (50 mM Tris-HCl, pH 7.5; 1 mM EDTA; 1 mM DTT) to a final conductivity equivalent to 50 mM NaCl (~8 mS/cm). This diluted sample, supplemented with protease inhibitor cocktail, was applied to a HiTrap Heparin HP 5 mL column, and the proteins were eluted using a linear gradient up to 2 M NaCl. The main peak fractions (~ 5 mL) were collected and subjected to further purification by gel filtration using an XK 16/70 Superose 6 PG column equilibrated with 50 mM Tris-HCl, pH 7.5, 200 mM NaCl, 1 mM EDTA, and 1 mM TCEP. The peak fractions were collected, concentrated using a Vivaspin 15 10K MWCO filter, flash frozen in liquid nitrogen, and stored at −80°C. Protein concentration was determined by absorbance, utilizing theoretical molar absorption and molecular weight values.

For the biotinylated *bsu*Smc(C119S, C437S, C826S, E1118Q, R643C) protein used in the sybody selection, the protein was first purified as described above, except that the reducing agent (TCEP) was omitted from the final gel filtration buffer. Labelling was performed by incubating 600 µL of *bsu*Smc(C119S, C437S, C826S, E1118Q, R643C) (83 µM in 50 mM Tris-HCl pH 7.5, 200 mM NaCl) with 1 mM PEG2-biotin maleimide for 10 minutes at 4 °C. The reaction was quenched by addition of 0.5 mM 2-mercaptoethanol. Excess label was removed using Zeba spin desalting columns (Thermo Fisher) in multiple parallel runs due to volume limitations. The final yield was 600 µL at 72.35 µM (subunit concentration). Labelled *bsu*Smc(C119S, C437S, C826S, E1118Q, R643C) was loaded onto a Superose 6 10/300 Increase column pre-equilibrated in 50 mM Tris-HCl pH 7.5, 200 mM NaCl. Peak fractions were pooled and mixed with ScpA and ScpB at a 1:1:2 molar ratio relative to the *bsu*Smc dimer. The final concentration of the full complex was adjusted to 5.7 µM. Complexes were aliquoted in 100 µL portions, flash-frozen in liquid nitrogen, and stored at −80 °C.

Purification of *bsu*ScpA

ScpA was purified using the method described by[25]. *E. coli* BL21-Gold (DE3) cells, transformed with a pET-28 derived plasmid encoding the ScpA protein, were used for expression. Cultivation was performed in ZYM-5052 autoinduction medium at 16°C for 28 hours. Cells were then harvested and resuspended in lysis buffer (50 mM Tris-HCl, pH 7.5; 200 mM NaCl; 5% glycerol) supplemented with protease inhibitor cocktail. The cells were lysed by sonication, and the lysate was clarified by centrifugation. The supernatant was applied to a 5 mL HiTrap Q ion exchange column and eluted with a gradient up to 2 M NaCl. Peak fractions were pooled and adjusted to a final concentration of 3 M NaCl by mixing with 4 M NaCl buffer. This mixture was loaded onto a HiTrap Butyl HP column and eluted with a reverse gradient to 50 mM NaCl. Eluted peak fractions were concentrated to 5 mL using Vivaspin 15 10K MWCO filters and further purified by size exclusion chromatography (SEC) on a HiLoad 16/600 Superdex 75 pg column equilibrated with 20 mM Tris-HCl, pH 7.5, and 200 mM NaCl. The purified protein was concentrated, flash frozen, and stored at −80°C.

Purification of *bsu*ScpB

ScpB was purified following the protocol outlined by [25]. The coding sequence of ScpB, cloned into a pET-22 derived plasmid, was transformed into chemically competent BL21-Gold (DE3) *E. coli* cells. These cells were cultivated in ZYM-5052 autoinduction medium at 24°C for 23 hours. Subsequently, the cells were harvested and resuspended in lysis buffer (50 mM Tris-HCl, pH 7.5; 150 mM NaCl; 1 mM EDTA; 1 mM DTT) supplemented with protease inhibitor cocktail. Cell lysis was performed by sonication, followed by centrifugation to remove cell debris. The resulting supernatant was diluted to a final NaCl concentration of 50 mM and loaded onto a 5 mL HiTrap Q HP column. Elution was achieved using a gradient up to 2 M NaCl. The eluate was then diluted with lysis buffer containing 4 M NaCl to achieve a final concentration of 3 M NaCl. This sample was applied to two 5 mL HiTrap Butyl columns connected in series, and the protein was eluted with a reverse gradient to 50 mM NaCl. The peak fractions from this column were concentrated and subjected to size exclusion chromatography (SEC) using a HiLoad 16/600 Superdex 200 pg column equilibrated with 50 mM Tris-HCl, pH 7.5, 100 mM NaCl, and 1 mM DTT. Fractions containing ScpB were concentrated, flash frozen, and stored at −80°C.

Medium scale sybody purification

Individual sybody plasmids were transformed into chemically competent *E. coli* MC1061 cells via heat shock at 42 °C for 45 s, followed by recovery in LB medium at 37 °C. Transformed cells were cultured overnight in TB medium supplemented with 25 µg/ml chloramphenicol. Precultures were used to inoculate 50 mL TB cultures, which were grown at 37 °C before shifting to 22 °C. Expression was induced with 0.02% (wt/vol) L-(+)-arabinose and continued overnight at 22 °C with shaking. Cells were harvested by centrifugation and resuspended in periplasmic extraction buffer. Following incubation at 4 °C, cells were pelleted, and the supernatant was supplemented with imidazole to 15 mM. The extract was incubated with His MultiTrap HP resin, followed by centrifugation and washing with TBS containing 30 mM imidazole. Elution was performed using

TBS with 300 mM imidazole. Purified sybodies were analyzed on a Sepax SRT-10C SEC100 column at 1 ml/min flow rate. Monomeric sybodies eluted between 11–12.5 ml, while retention volumes <11 ml indicated oligomerization, and >14 ml suggested strong column interaction. Non-expressed, oligomeric, or highly interacting sybodies were discarded. Typical yields ranged from 200 µg to 1 mg [16].

Fluorescence imaging of ParB-GFP strains Image acquisition

B. subtilis cells were first cultured in LB supplemented with 5 µg/mL chloramphenicol and 0.5% glucose at 30°C, from which a day culture was inoculated to 0.005 in LB with 5 µg/mL chloramphenicol. When needed, cultures were induced at OD_{600} ~ 0.02 with 0.5% xylose and grown an extra 30 minutes until imaging at an OD_{600} of 0.04. For microscopy analysis, 0.5 µL of the cell suspension was spotted onto agarose-coated microscopy slides. Images were acquired using a Leica DMi8 microscope equipped with an sCMOS DFC9000 (Leica) camera, a SOLA light engine (Lumencor), and a 100×/1.40 oil-immersion objective. Exposure time for image acquisition was set to 600 ms. Acquired images were processed using LAS X Office software (v.1.4.7.28982, Leica Microsystems).

Image analysis

Microscopy images were analyzed using a fully automated image processing pipeline. Cell segmentation was performed with the pretrained Omnipose model[30] implemented in Cellpose[31], which is optimized for bacterial morphologies. Prior to segmentation, a normalization step was applied to standardize image contrast. Following segmentation, intracellular foci were detected using Spotiflow[32], a dedicated model trained for spot identification. Each detected spot was assigned to an individual cell based on spatial location, enabling quantification of the number of foci per cell. Cell morphology analysis was also performed to estimate cell length.

Quantitative results were compiled into a structured dataset, including the number of cells per image, percentage of cells lacking foci, number of foci per cell, cell length, and number of foci per micron. Data visualization and statistical analysis was performed using GraphPad Prism 10.4.1 (627).

ELISA

E. coli MC1061 colonies were screened for sybody expression, and periplasmic extracts were obtained as per the original protocol [16]. ELISA plates were coated with Protein A and anti-c-Myc antibody before incubation with sybody-containing extracts. Three wells per sybody were incubated with biotinylated maltose binding protein (MBP, negative control) or with 50 nM biotinylated bsSmc-ScpAB(E1118Q) with ATP/dsDNA or without. Washes and ELISA development were performed using TBSM-D. Absorbance was measured at 650 nm.

ATPase measurements

ATPase activity was assessed using the coupled pyruvate kinase/lactate dehydrogenase reaction as described by [14]. ADP production was monitored over a period of 1 hour by measuring the absorbance changes of NADH at 340 nm. Data collection was performed using a Synergy Neo Hybrid Multi-Mode Microplate Reader. The reaction mixture comprised 1 mM NADH, 3 mM phosphoenolpyruvic acid, 100 U pyruvate kinase, 20 U lactate dehydrogenase, and varying concentrations of ATP. For assays requiring double-stranded oligonucleotides, a 40 bp oligonucleotide (5'-TTAGTTGTTC GTAGTGCTCG TCTGGCTCTG GATTACCCGC-3') was added to a final concentration of 3 mM. The final protein concentration in the assay was 0.15 µM *bsu*Smc dimers in ATPase assay buffer (50 mM HEPES-KOH, pH 7.5; 50 mM NaCl; 2 mM MgCl2). All measurements were conducted at 25°C.

Supplementary figures

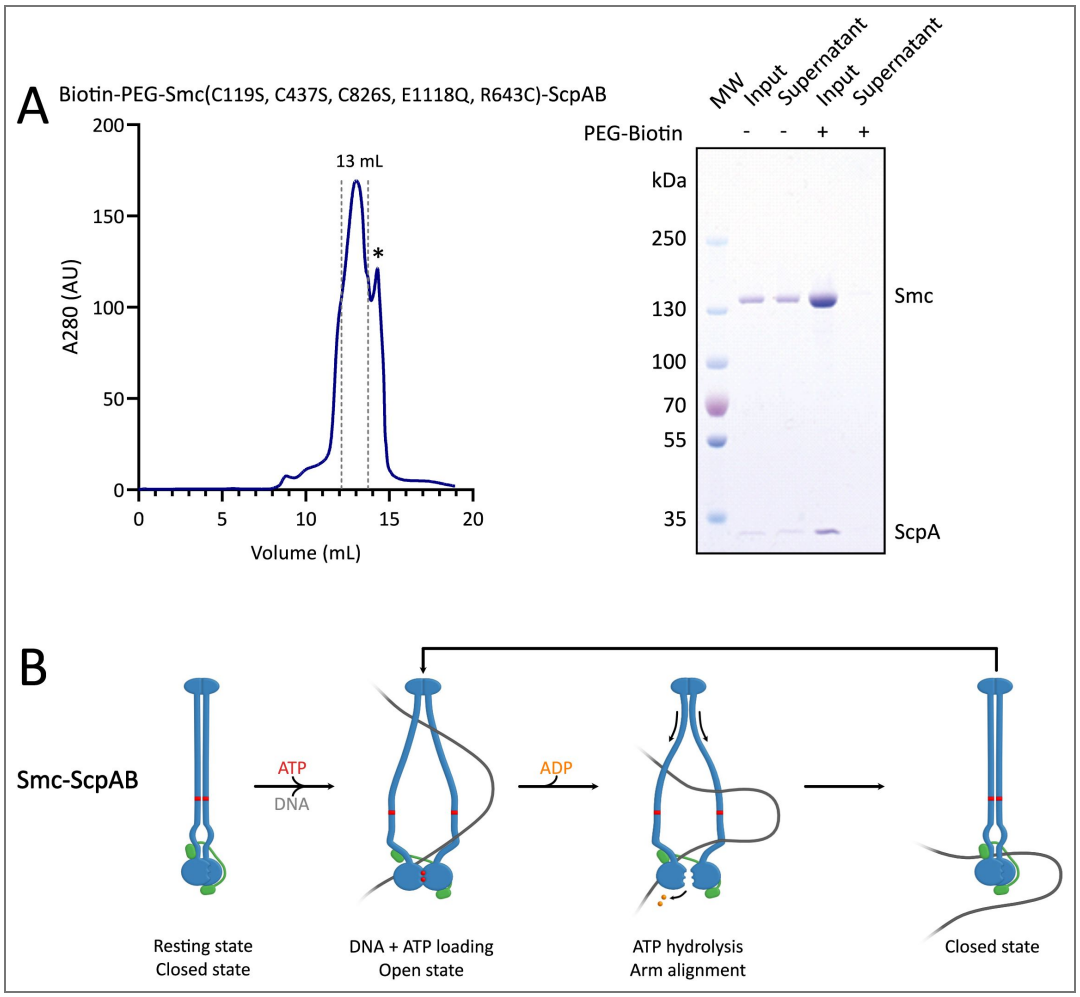

Figure S1. Preparation of *bsu*Smc(C119S, C437S, C826S, E1118Q, R643C)-ScpAB complex and loop extrusion model (A) Size-exclusion chromatography profile of biotinylated *bsu*Smc(C119S, C437S, C826S, E1118Q, R643C)-ScpAB complex. Peak fractions (elution at ~13 mL, pooled fractions indicated by dotted lines for a final volume of 1.8 mL) were collected for downstream use; the final concentration was 5.9 µM (dimer). * : A secondary peak appeared at ~14 mL; its identity was uncertain and was excluded from the peak. SDS-PAGE confirms successful biotinylation of the *bsu*Smc(C119S, C437S, C826S, E1118Q, R643C)-ScpAB complex. **(B)** Segment-capture model for *bsu*Smc-ScpAB, in which ATP binding and hydrolysis drive transitions between open and closed conformations to mediate loop extrusion.

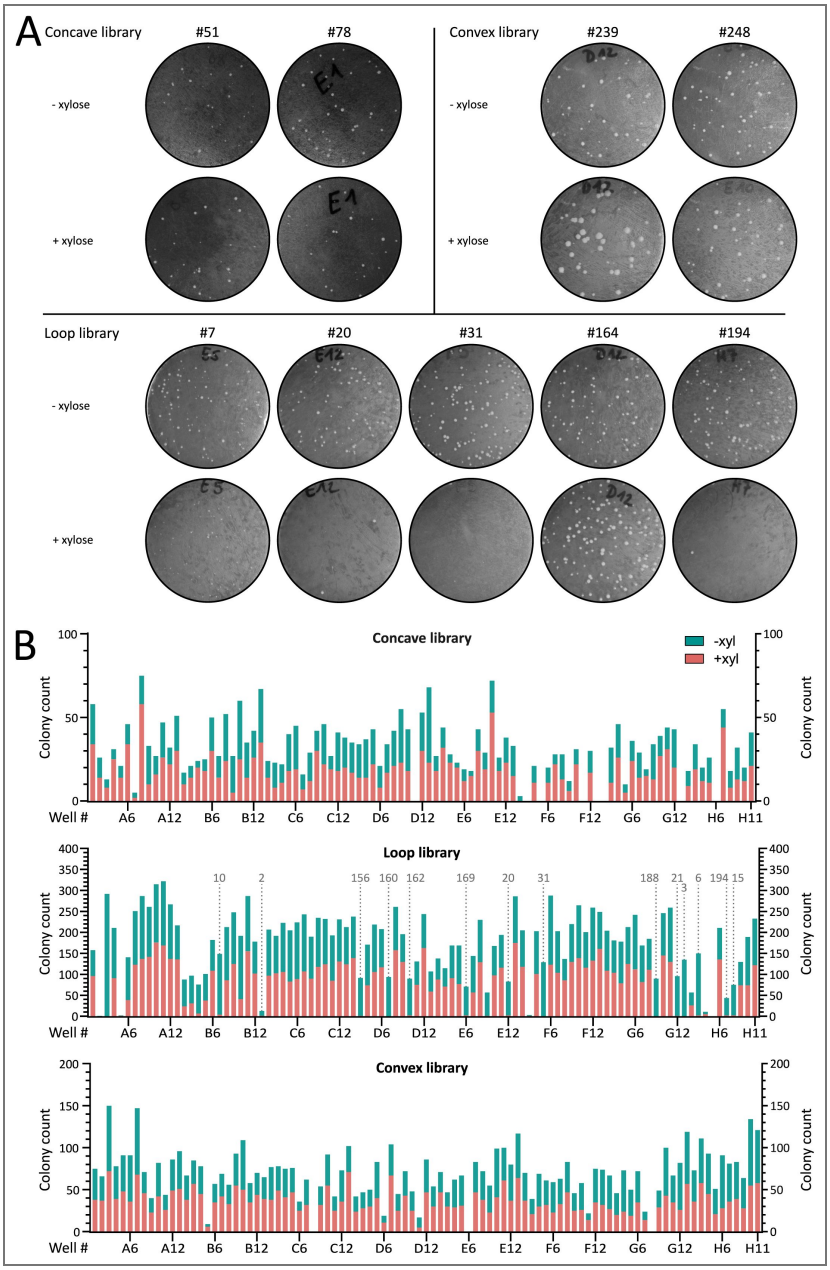

Figure S2. Representative results from *in vivo* sybody selection based on colony formation.

(A) Representative examples of *in vivo* transformation assays for nine sybody-expressing *B. subtilis* strains. Sybody genes were integrated into the *amyE* locus under xylose-inducible control. Transformants were grown on oxoid nutrient agar (ONA) plates supplemented with chloramphenicol and 0.5% xylose to assess growth defects. Shown are candidates from the concave library: Sb051 (well B08) and Sb078 (D12). Loop library: Sb007 (E05), Sb020 (E12), Sb031 (F05), Sb164 (D12) and NbH07 (Sb194). Convex library: Sb239 (D12) and Sb248 (E10). **(B)** Growth assay results for the 285 *B. subtilis* strains expressing individual xylose-inducible sybodies. Bars show each colony counts “without” (green) on top of “with” (pink) xylose. Strains are ordered by their original 96-well plate. Only the loop library yielded sybodies that consistently impaired growth under inducing conditions (dotted line). Sybody numbers indicated above the plots correspond to positive candidates used in subsequent experiments, numbered according to order of use. Notably, the strain corresponding to the E09 M sybody (Sb018), also showed an absence of growth upon sybody induction. However, this sybody candidate gave intermediate phenotypes in later experiments, which is why it was excluded from this study. Results for the loop library are also shown in Figure 1.

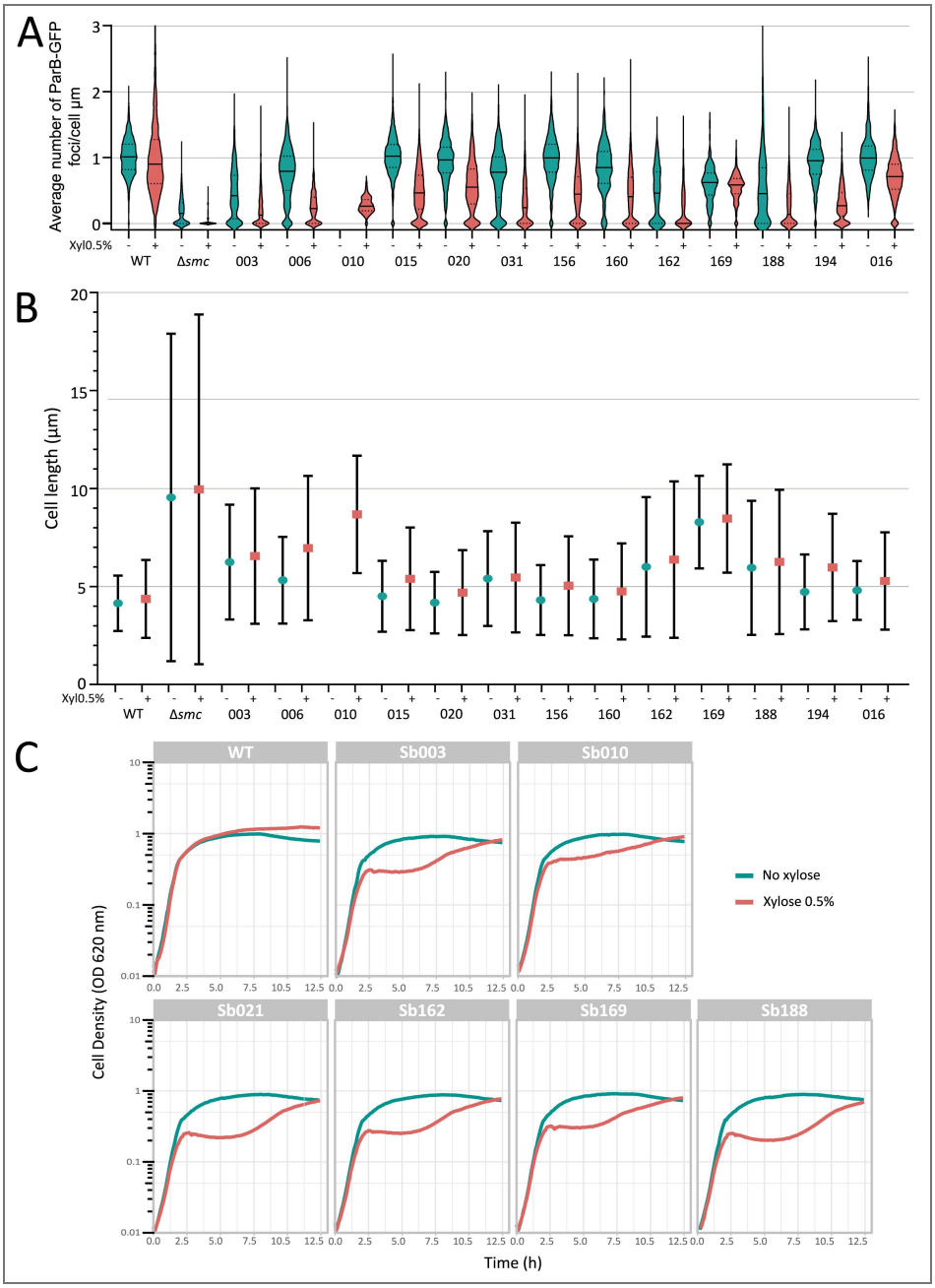

Figure S3. Functional impact of sybody expression on chromosome organization, cell length, and growth in *B. subtilis*.

(A) Average number of ParB-GFP foci per µm of cell length in strains expressing individual sybodies, with and without xylose induction. Most uninduced strains differed significantly from the Smc WT control, likely due to leaky expression from the P_{xyl} ($p < 0.0001$), except Sb015 ($p > 0.9999$), Sb156 ($p = 0.2345$), and Sb016 (negative control, $p > 0.9999$). **(B)** Average cell length across the same conditions, measured in ParB-GFP strains with or without Smc, and with or without each sybody. Bars indicate standard deviation. Tested sybodies caused cell elongation, a characteristic phenotype of impaired Smc activity, as chromosome segregation defects delay cell division, with mean lengths from 4.70 ± 2.16 µm (Sb020) to 8.68 ± 2.99 µm (Sb010), compared to 4.51 ± 1.95 µm in wild-type and 9.96 ± 8.92 µm in Δ*smc*. **(C)** Growth curves of *B. subtilis* strains expressing individual sybodies compared to the WT strain, with and without xylose induction. Each curve represents the mean of two biological replicates. Six sybodies were randomly picked and showed in this figure. Fluorophore-free strains showed wild type-like growth without xylose but strong delays post-induction, followed by partial growth recovery after 12 hours, likely due to xylose depletion or suppressor emergence. In sybody-expressing strains, a clear drop in cell density was observed ~2.5 hours post-induction.

Figure S4. Sybody-GFP expression at different inducer concentration

(A) Selected Sybody-GFP proteins were tested by GFP imaging at different inducer concentrations (0, 0.005, 0.05 and 0.5 % xylose). Representative images are shown. Notably, sybody Sb007 (E5, loop library) generates a mild growth phenotype (smaller colonies but normal colony numbers, Figure 1A and 1B) but shows good expression levels and focal localization (top row).

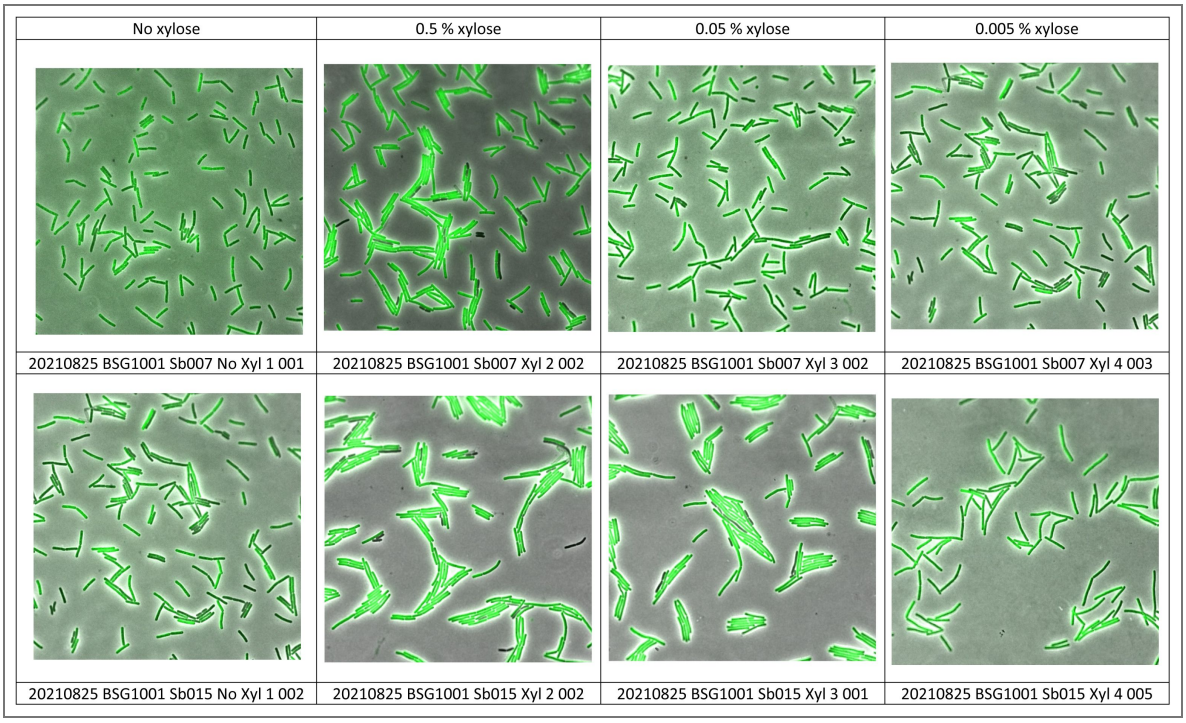

Figure S5. Imaging of various Sybody-GFP proteins without inducer.

(A) Selected Sybody-GFP constructs were grown in the absence of inducer and tested for gfp expression. Representative images are shown.

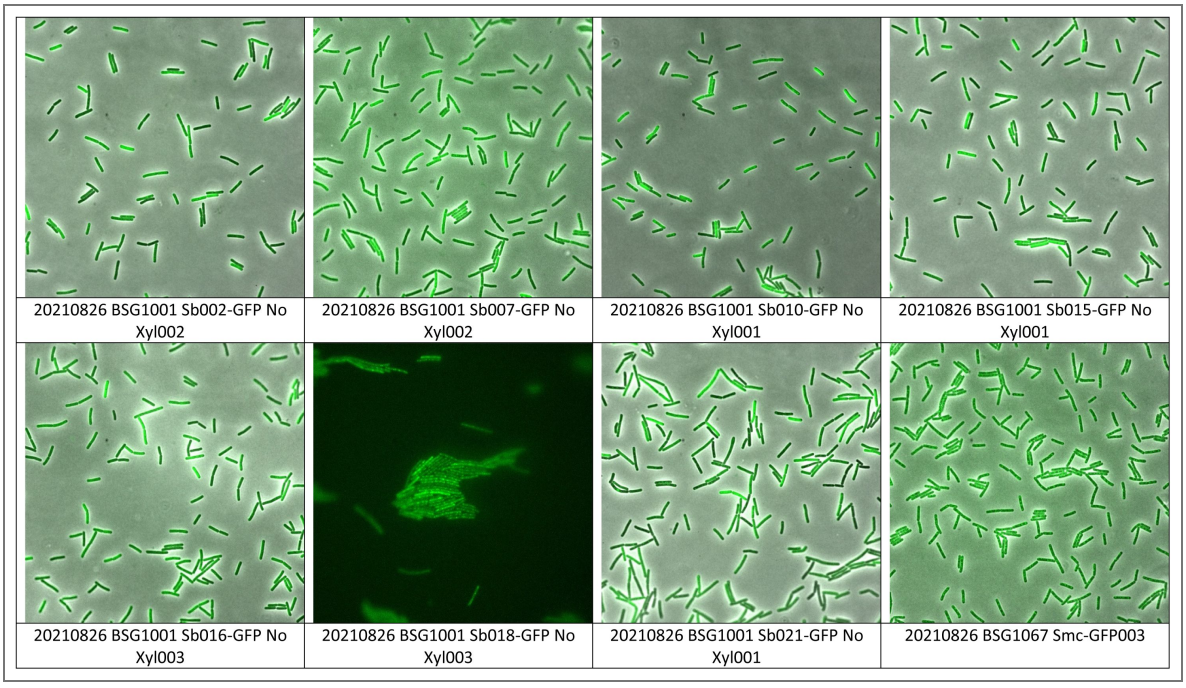

Figure S6. ATPase hydrolysis rate of the *bsu*Smc-ScpAB complex with each selected sybody and viability of *B. subtilis* strains expressing chimeric Smc-ScpAB complexes in the absence of sybody induction.

(A) Spotting assay assessing the growth of *B. subtilis* strains carrying chimeric Smc-ScpAB operons composed of *S. pneumoniae* and *B. subtilis* components. Strains harbor individual sybody constructs integrated at the *amyE* locus under control of a xylose-inducible promoter but were grown without inducer. "–" indicates no integration at *amyE*; "EV" corresponds to an empty vector control containing only the chloramphenicol resistance cassette. Numbered labels indicate strains carrying specific sybody constructs. Cells were spotted on rich medium (ONA) containing chloramphenicol and incubated for 16 h at 37 °C. **(B)** Overall ATPase hydrolysis rate of the *bsu*Smc-ScpAB complex in presence of each sybody and +/-DNA. Sb06, 021 and 194 triggered a significant difference in ATP hydrolysis between +/- dsDNA conditions. The rest is non-significant.

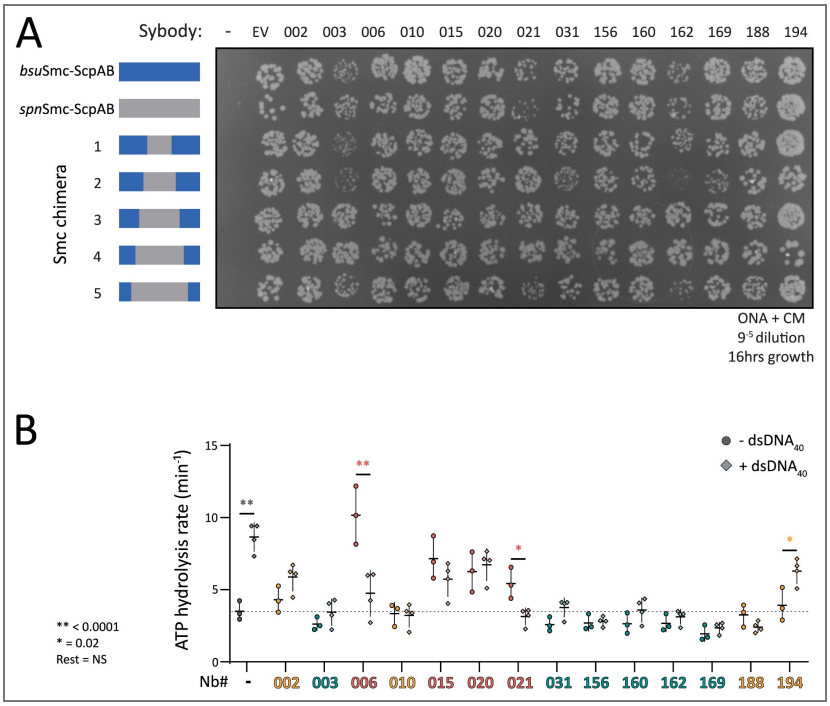

Figure S7. Hypothetical model for an Opening^{DOWN} class of sybodies, not recovered in this study.

This may indicate that stabilizing an open conformation near the ATPase heads does not interfere with Smc function.

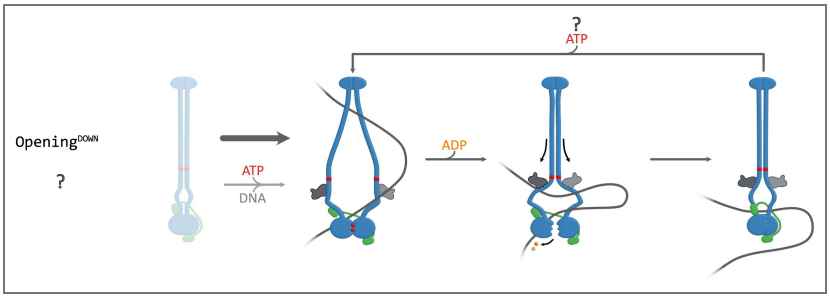

Data availability

All raw data will be made available at Mendeley Data DOI: 10.17632/k6k62p7z2s.1 (*https://data.mendeley.com/datasets/k6k62p7z2s/1*).

Acknowledgements

We are grateful to Roberto Vazquez Nunez for the biotinylated *bsu*Smc(C119S, C437S, C826S, E1118Q, R643C) protein preparation, Arianna Ravera from the DCSR computing facility for help in image analysis and data extraction of the fluorescence microscopy images. Members of the Gruber Lab for critical feedback of the manuscript and for stimulating discussions.

Additional information

Funding

This study was supported by internal funding and by the European Research Council (Horizon 2020 ERC CoG 724482).

Author contributions

O.G. performed all *in vivo* experiments from sybody selection, fluorescence microscopy imaging, chimeric phenotypic screen. M.T. and L.H-H. performed the *in vitro* sybody screening (ribosome display, phage display, and first sybody purification). O.G. performed protein purifications, cross-linking and ATPase measurements, as well as data analysis, figures and writing. O.G. wrote the first manuscript draft. All authors reviewed and edited the manuscript. Funding acquisition and supervision, S.G.

Funding

Funder	Grant reference number	Author
EC | Horizon Europe | Excellent Science | HORIZON EUROPE European Research Council (ERC)	https://doi.org/10.3030/724482	Stephan Gruber

Author ORCID iDs

Ophélie Gosselin: https://orcid.org/0009-0004-8996-4689
Michael Taschner: https://orcid.org/0000-0002-8881-3705
Lea M Huber-Hürlimann: https://orcid.org/0000-0001-9907-7830
Markus A Seeger: https://orcid.org/0000-0003-1761-8571
Stephan Gruber: https://orcid.org/0000-0002-0150-0395

Additional files

Table S1. ELISA sybody binding assay.

Table S2. Sybody sequences.

Table S3. Percentage of cells lacking ParB-GFP foci, indicating the absence of chromosome due to segregation defect. In presence and absence of xylose for sybody induction.

Tables S4–S6. **Table S4.** Strains. **Table S5.** Plasmids. **Table S6.** Oligonucleotides.

References

1. **Zimmermann I.**, Egloff P., Hutter C.A., Arnold F.M., Stohler P., Bocquet N., Hug M.N., Huber S., Siegrist M., Hetemann L., *et al.* (2018) Synthetic single domain antibodies for the conformational trapping of membrane proteins. *eLife* **7** https://doi.org/10.7554/eLife.34317 | PubMed

2. **Pacesa M.,** Nickel L., Schellhaas C., Schmidt J., Pyatova E., Kissling L., Barendse P., Choudhury J., Kapoor S., Alcaraz-Serna A., *et al.* (2025) One-shot design of functional protein binders with BindCraft. *Nature* **646**:483-492 https://doi.org/10.1038/s41586-025-09429-6 | PubMed
3. **Yatskevich S.,** Rhodes J., Nasmyth K (2019) Organization of Chromosomal DNA by SMC Complexes. *Annu Rev Genet* **53**:445-482 https://doi.org/10.1146/annurev-genet-112618-043633 | PubMed
4. **Burmann F.,** Gruber S (2015) SMC condensin: promoting cohesion of replicon arms. *Nat Struct Mol Biol* **22**:653-655 https://doi.org/10.1038/nsmb.3082 | PubMed
5. **Gruber S.,** Errington J (2009) Recruitment of condensin to replication origin regions by ParB/SpoOJ promotes chromosome segregation in B. subtilis. *Cell* **137**:685-696 https://doi.org/10.1016/j.cell.2009.02.035 | PubMed
6. **Wang X.,** Tang O.W., Riley E.P., Rudner D.Z (2014) The SMC condensin complex is required for origin segregation in Bacillus subtilis. *Curr Biol* **24**:287-292 https://doi.org/10.1016/j.cub.2013.11.050 | PubMed
7. **Liu H.W.,** Roisne-Hamelin F., Taschner M., Collier J., Srinivasan M., Gruber S (2025) The SMC Hinge is a Selective Gate for Obstacle Bypass. *Nat Commun* **16** https://doi.org/10.1038/s41467-025-65408-5 | PubMed
8. **Sullivan N.L.,** Marquis K.A., Rudner D.Z (2009) Recruitment of SMC by ParB-parS organizes the origin region and promotes efficient chromosome segregation. *Cell* **137**:697-707 https://doi.org/10.1016/j.cell.2009.04.044 | PubMed
9. **Diebold-Durand M.L.,** Lee H., Ruiz Avila L.B., Noh H., Shin H.C., Im H., Bock F.P., Burmann F., Durand A., Basfeld A., *et al.* (2017) Structure of Full-Length SMC and Rearrangements Required for Chromosome Organization. *Mol Cell* **67**:334-347.e335. https://doi.org/10.1016/j.molcel.2017.06.010 | PubMed
10. **Marko J.F.,** De Los Rios P., Barducci A., Gruber S. (2019) DNA-segment-capture model for loop extrusion by structural maintenance of chromosome (SMC) protein complexes. *Nucleic Acids Res* **47**:6956-6972 https://doi.org/10.1093/nar/gkz497 | PubMed
11. **Minnen A.,** Burmann F., Wilhelm L., Anchimiuk A., Diebold-Durand M.L., Gruber S (2016) Control of Smc Coiled Coil Architecture by the ATPase Heads Facilitates Targeting to Chromosomal ParB/parS and Release onto Flanking DNA. *Cell Rep* **14**:2003-2016 https://doi.org/10.1016/j.celrep.2016.01.066 | PubMed
12. **Rasmussen S.G.,** Choi H.J., Fung J.J., Pardon E., Casarosa P., Chae P.S., Devree B.T., Rosenbaum D.M., Thian F.S., Kobilka T.S., *et al.* (2011) Structure of a nanobody-stabilized active state of the beta(2) adrenoceptor. *Nature* **469**:175-180 https://doi.org/10.1038/nature09648 | PubMed
13. **Vazquez Nunez R,** Polyhach Y., Soh Y.M., Jeschke G., Gruber S. (2021) Gradual opening of Smc arms in prokaryotic condensin. *Cell Rep* **35**:109051 https://doi.org/10.1016/j.celrep.2021.109051 | PubMed
14. **Burmann F.,** Basfeld A., Vazquez Nunez R., Diebold-Durand M.L., Wilhelm L., Gruber S (2017) Tuned SMC Arms Drive Chromosomal Loading of Prokaryotic Condensin. *Mol Cell* **65**:861-872.e869. https://doi.org/10.1016/j.molcel.2017.01.026 | PubMed
15. **Hirano M.,** Hirano T (2004) Positive and negative regulation of SMC-DNA interactions by ATP and accessory proteins. *EMBO J* **23**:2664-2673 https://doi.org/10.1038/sj.emboj.7600264 | PubMed
16. **Zimmermann I.,** Egloff P., Hutter C.A.J., Kuhn B.T., Brauer P., Newstead S., Dawson R.J.P., Geertsma E.R., Seeger M.A. (2020) Generation of synthetic nanobodies against delicate proteins. *Nat Protoc* **15**:1707-1741 https://doi.org/10.1038/s41596-020-0304-x | PubMed
17. **Deneka D.,** Rutz S., Hutter C.A.J., Seeger M.A., Sawicka M., Dutzler R (2021) Allosteric modulation of LRRC8 channels by targeting their cytoplasmic domains. *Nat Commun* **12** https://doi.org/10.1038/s41467-021-25742-w | PubMed
18. **Diebold-Durand M.L.,** Burmann F., Gruber S (2019) High-Throughput Allelic Replacement Screening in Bacillus subtilis. *Methods Mol Biol* **2004**:49-61 https://doi.org/10.1007/978-1-4939-9520-2_5 | PubMed

19. **Hutter C.A.J.,** Timachi M.H., Hurlimann L.M., Zimmermann I., Egloff P., Goddeke H., Kucher S., Stefanic S., Karttunen M., Schafer L.V., *et al.* (2019) The extracellular gate shapes the energy profile of an ABC exporter. *Nat Commun* **10**:2260 https://doi.org/10.1038/s41467-019-09892-6 | PubMed

20. **Gruber S.,** Veening J.W., Bach J., Blettinger M., Bramkamp M., Errington J (2014) Interlinked sister chromosomes arise in the absence of condensin during fast replication in B. subtilis. *Curr Biol* **24**:293-298 https://doi.org/10.1016/j.cub.2013.12.049 | PubMed

21. **Bock F.P.,** Liu H.W., Anchimiuk A., Diebold-Durand M.L., Gruber S (2022) A joint-ParB interface promotes Smc DNA recruitment. *Cell Rep* **40**:111273 https://doi.org/10.1016/j.celrep.2022.111273 | PubMed

22. **Gabler F.,** Nam S.Z., Till S., Mirdita M., Steinegger M., Soding J., Lupas A.N., Alva V (2020) Protein Sequence Analysis Using the MPI Bioinformatics Toolkit. *Curr Protoc Bioinformatics* **72**:e108 https://doi.org/10.1002/cpbi.108 | PubMed

23. **Jumper J.,** Evans R., Pritzel A., Green T., Figurnov M., Ronneberger O., Tunyasuvunakool K., Bates R., Zidek A., Potapenko A., *et al.* (2021) Highly accurate protein structure prediction with AlphaFold. *Nature* **596**:583-589 https://doi.org/10.1038/s41586-021-03819-2 | PubMed

24. **Soh Y.M.,** Burmann F., Shin H.C., Oda T., Jin K.S., Toseland C.P., Kim C., Lee H., Kim S.J., Kong M.S., *et al.* (2015) Molecular basis for SMC rod formation and its dissolution upon DNA binding. *Mol Cell* **57**:290-303 https://doi.org/10.1016/j.molcel.2014.11.023 | PubMed

25. **Vazquez Nunez R.,** Ruiz Avila L.B., Gruber S. (2019) Transient DNA Occupancy of the SMC Interarm Space in Prokaryotic Condensin. *Mol Cell* **75**:209-223.e206. https://doi.org/10.1016/j.molcel.2019.05.001 | PubMed

26. **Seeger M.A.,** Mittal A., Velamakanni S., Hohl M., Schauer S., Salaa I., Grutter M.G., van Veen H.W. (2012) Tuning the drug efflux activity of an ABC transporter in vivo by in vitro selected DARPin binders. *PLoS One* **7**:e37845 https://doi.org/10.1371/journal.pone.0037845 | PubMed

27. **Kruse A.C.,** Ring A.M., Manglik A., Hu J., Hu K., Eitel K., Hubner H., Pardon E., Valant C., Sexton P.M., *et al.* (2013) Activation and allosteric modulation of a muscarinic acetylcholine receptor. *Nature* **504**:101-106 https://doi.org/10.1038/nature12735 | PubMed

28. **Burmann F.,** Shin H.C., Basquin J., Soh Y.M., Gimenez-Oya V., Kim Y.G., Oh B.H., Gruber S (2013) An asymmetric SMC-kleisin bridge in prokaryotic condensin. *Nat Struct Mol Biol* **20**:371-379 https://doi.org/10.1038/nsmb.2488 | PubMed

29. **Denereaz J.,** Veening J.W (2024) BactEXTRACT: an R Shiny app to quickly extract, plot and analyse bacterial growth and gene expression data. *Access Microbiol* **6** https://doi.org/10.1099/acmi.0.000742.v3 | PubMed

30. **Cutler K.J.,** Stringer C., Lo T.W., Rappez L., Stroustrup N., Brook Peterson S., Wiggins P.A., Mougous J.D (2022) Omnipose: a high-precision morphology-independent solution for bacterial cell segmentation. *Nat Methods* **19**:1438-1448 https://doi.org/10.1038/s41592-022-01639-4 | PubMed

31. **Stringer C.,** Wang T., Michaelos M., Pachitariu M (2021) Cellpose: a generalist algorithm for cellular segmentation. *Nat Methods* **18**:100-106 https://doi.org/10.1038/s41592-020-01018-x | PubMed

32. **Mantes Dominguez,** Herrera A., Khven A., Schlaeppi I., Kyriacou A., Tsissios E., Skoufa G., Santangeli E., Buglakova L., Durmus E., *et al.* (2025) Spotiflow: accurate and efficient spot detection for fluorescence microscopy with deep stereographic flow regression. *Nat Methods* **22**:1495-1504 https://doi.org/10.1038/s41592-025-02662-x | PubMed

Peer reviews

Reviewer #1 (Public review):

[Editors' note: this version has been assessed by the Reviewing Editor without further input from the original reviewers. The authors have addressed the major comments raised in the

previous round of review. Public Reviews below refer to the version submitted to Review Commons.]

Summary:

Gosselin et al., develop a method to target protein activity using synthetic single-domain nanobodies (sybodies). They screen a library of sybodies using ribosome/ phage display generated against bacillus Smc-ScpAB complex. Specifically, they use an ATP hydrolysis deficient mutant of SMC so as to identify sybodies that will potentially disrupt Smc-ScpAB activity. They next screen their library in vivo, using growth defects in rich media as a read-out for Smc activity perturbation. They identify 14 sybodies that mirror smc deletion phenotype including defective growth in fast-growth conditions, as well as chromosome segregation defects. The authors use a clever approach by making chimeras between bacillus and S. pnuemoniae Smc to narrow-down to specific regions within the bacillus Smc coiled-coil that are likely targets of the sybodies. Using ATPase assays, they find that the sybodies either impede DNA-stimulated ATP hydrolysis or hyperactivate ATP hydrolysis (even in the absence of DNA). The authors propose that the sybodies may likely be locking Smc-ScpAB in the "closed" or "open" state via interaction with the specific coiled-coil region on Smc. I have a few comments that the authors should consider:

Major comments:

(1) Lack of direct in vitro binding measurements:

The authors do not provide measurements of sybody affinities, binding/ unbinding kinetics, stoichiometries with respect to Smc-ScpAB. Additionally, do the sybodies preferentially interact with Smc in ATP/ DNA-bound state? And do the sybodies affect the interaction of ScpAB with SMC?

It is understandable that such measurements for 14 sybodies is challenging, and not essential for this study. Nonetheless, it is informative to have biochemical characterization of sybody interaction with the Smc-ScpAB complex for at least 1-2 candidate sybodies described here.

(2) Many modes of sybody binding to Smc are plausible

The authors provide an elaborate discussion of sybodies locking the Smc-ScpAB complex in open/ closed states. However, in the absence of structural support, the mechanistic inferences may need to be tempered. For example, is it also not possible for the sybodies to bind the inner interface of the coiled-coil, resulting in steric hinderance to coiled-coil interactions. It is also possible that sybody interaction disrupts ScpAB interaction (as data ruling this possibility out has not been provided). Thus, other potential mechanisms would be worth considering/ discussing. In this direction, did AlphaFold reveal any potential insights into putative binding locations?

(3) Sybody expression in vivo

Have the authors estimated sybody expression in vivo? Are they all expressed to similar levels?

(4) Sybodies should phenocopy ATP hydrolysis mutant of Smc

The sybodies were screened against an ATP hydrolysis deficient mutant of Smc, with the rationale that these sybodies would interfere this step of the Smc duty cycle. Does the expression of the sybodies in vivo phenocopy the ATP hydrolysis deficient mutant of Smc? Could the authors consider any phenotypic read-outs that can indicate whether the sybody action results in an smc-null effect or specifically an ATP hydrolysis deficient effect?

Significance:

Overall, this is an impressive study that uses an elegant strategy to find inhibitors of protein activity in vivo. The manuscript is clearly written and the experiments are logical and well-designed. The findings from the study will be significant to the broad field of genome biology, synthetic biology and also SMC biology. Specifically, the coiled coil domain of SMC proteins has been proposed to be of high functional value. The authors have elegantly identified key coiled-coil regions that may be important for function, and parallelly exhibited potential of the use of synthetic sybody/designed binders for inhibition of protein activity.

https://doi.org/10.7554/eLife.111131.2.sa3

Reviewer #2 (Public review):

Summary:

Structural Maintenance of Chromosome proteins (SMCs), a family of proteins found in almost all organisms, are organizers of DNA. They accomplish this by a process known as loop extrusion, wherein double-stranded DNA is actively reeled in and extruded into loops. Although SMCs are known to have several DNA binding regions, the exact mechanism by which they facilitate loop extrusion is not understood but is believed to entail large conformational changes. There are currently several models for loop extrusion, including one wherein the coiled coil (CC) arms open, but there is a lack of insightful experimentation and analysis to confirm any of these models. The work presented aims to provide much-needed new tools to investigate these questions: conformation-selective sybodies (synthetic nanobodies) that are likely to alter the CC opening and closing reactions.

The authors produced, isolated, and expressed sybodies that specifically bound to Bacillus subtilis Smc-ScpAB. Using chimeric Smc constructs, where the coiled coils were partly replaced with the corresponding sequences from Streptococcus pneumoniae, the authors revealed that the isolated sybodies all targeted the same 4N CC element of the Smc arms. This region is likely disrupted by the sybodies either by stopping the arms from opening (correctly) or forcing them to stay open (enough). Disrupting these functional elements is suggested to cause the Smc-dependent chromosome organization lethal phenotype, implying that arm opening and closing is a key regulatory feature of bacterial Smc-ScpAB.

Significance:

The authors present a new method for trapping bacterial Smc's in certain conformations using synthetic antibodies. Using these antibodies, they have pinpointed the (previously suggested) 4N region of the coiled coils as an essential site for the opening and closing of the Smc coiled coil arms and that hindering these reactions blocks Smc-driven chromosomal organization. The work has important implications for how we might elucidate the mechanism of DNA loop extrusion by SMC complexes.

https://doi.org/10.7554/eLife.111131.2.sa2

Reviewer #3 (Public review):

Summary:

Gosselin et al. use the sybody technology to study effects of in vivo inhibition of the Bacillus subtilis SMC complex. Smc proteins are central DNA binding elements of several complexes that are vital for chromosome dynamics in almost all organisms. Sybodies are selected from three different libraries of the single domain antibodies, using the "transition state" mutant Smc. They identify 14 such mutant sybodies that are lethal when expressed in vivo, because they prevent proper function of Smc. The authors present evidence suggesting that all

obtained sybodies bind to a coiled-coil region close to the Smc "neck", and thereby interfere with the Smc activity cycle, as evidenced by defective ATPase activity when Smc is bound to DNA.

The study is well done and presented and shows that the strategy is very potent in finding a means to quickly turn off a protein's function in vivo, much quicker than depleting the protein.

The authors also draw conclusions on the molecular mode of action of the SMC complex. The provide a number of suggestive experiments, but in my view mostly indirect evidence for such mechanism.

My main criticism is that the authors have used a single - and catalytically trapped form of SMC. They speculate why they only obtain sybodies from one library, and then only identify sybodies that bind to a rather small part of the large Smc protein. While the approach is definitely valuable, it is biassed towards sybodies that bind to Smc in a quite special way, it seems. Using wild type Smc would be interesting, to make more robust statements about the action of sybodies potentially binding to different parts of Smc.

Line 105: Alternatively, the other libraries did not produce good binders or these sybodies were 106 not stably expressed in B. subtilis. This could be tested using Western blotting - I am assuming sybody antibodies are commercially available. However, this test is not important for the overall study, it would just clarify a minor point.

Fig. 2B: is odd to count Spo0J foci per cells, as it is clear from the images that several origins must be present within the fluorescent foci. I am fine with the "counting" method, as the images show there is a clear segregation defect when sybodies are expressed, I believe the authors should state, though, that this is not a replication block, but failure to segregate origins.

Testing binding sites of sybodies to the SMC complex is done in an indirect manner, by using chimeric Smc constructs. I am surprised why the authors have not used in vitro crosslinking: the authors can purify Smc, and mass spectrometry analyses would identify sites where sybodies are crosslinked to Smc. Again, I am fine with the indirect method, but the authors make quite concrete statements on binding based on non-inhibition of chimeric Smc; I can see alternative explanations why a chimera may not be targeted.

Smc-disrupting sybodies affect the ATPase activity in one of two ways. Again, rather indirect experiments. This leads to the point Revealing Smc arm dynamics through synthetic binders in the discussion. The authors are quite careful in stating that their experiments are suggestive for a certain mode of action of Smc, which is warranted.

In line 245, they state More broadly, the study demonstrates how synthetic binders can trap, stabilize, or block transient conformations of active chromatin-associated machines, providing a powerful means to probe their mechanisms in living cells. This is off course a possible scenario for the use of sybodies, but the study does not really trap Smc in a transient conformation, at least this is not clearly shown.

Overall, it is an interesting study, with a well-presented novel technology, and a limited gain of knowledge on SMC proteins.

Significance:

The work describes the gaining and use of single-binder antibodies (sybodies) to interfere with the function of proteins in bacteria. Using this technology for the SMC complex, the authors demonstrate that they can obtain a significant of binders that target a defined region is SMC and thereby interfere with the ATPase cycle.

The study does not present a strong gain of knowledge of the mode of action of the SMC complex.

https://doi.org/10.7554/eLife.111131.2.sa1

Author response:

The following is the authors' response to the original reviews

> ***Public Reviews:***
>
> ***Reviewer #1 (Public review):***
>
> *Summary:*
>
> *Gosselin et al., develop a method to target protein activity using synthetic single-domain nanobodies (sybodies). They screen a library of sybodies using ribosome/ phage display generated against bacillus Smc-ScpAB complex. Specifically, they use an ATP hydrolysis deficient mutant of SMC so as to identify sybodies that will potentially disrupt Smc-ScpAB activity. They next screen their library in vivo, using growth defects in rich media as a read-out for Smc activity perturbation. They identify 14 sybodies that mirror smc deletion phenotype including defective growth in fast-growth conditions, as well as chromosome segregation defects. The authors use a clever approach by making chimeras between bacillus and S. pnuemoniae Smc to narrow-down to specific regions within the bacillus Smc coiled-coil that are likely targets of the sybodies. Using ATPase assays, they find that the sybodies either impede DNA-stimulated ATP hydrolysis or hyperactivate ATP hydrolysis (even in the absence of DNA). The authors propose that the sybodies may likely be locking Smc-ScpAB in the "closed" or "open" state via interaction with the specific coiled-coil region on Smc. I have a few comments that the authors should consider:*
>
> *Major comments:*
>
> *(1) Lack of direct in vitro binding measurements:*
>
> *The authors do not provide measurements of sybody affinities, binding/ unbinding kinetics, stoichiometries with respect to Smc-ScpAB. Additionally, do the sybodies preferentially interact with Smc in ATP/ DNA-bound state? And do the sybodies affect the interaction of ScpAB with SMC?*
>
> *It is understandable that such measurements for 14 sybodies is challenging, and not essential for this study. Nonetheless, it is informative to have biochemical characterization of sybody interaction with the Smc-ScpAB complex for at least 1-2 candidate sybodies described here.*

We agree with the reviewer that adding such data would be reassuring and that obtaining solid data using purified components is not trivial, even for a smaller selection of sybodies. We have now incorporated ELISA data as new Table S1, which shows that most sybodies support clear binding to Smc-ScpAB. Curiously, while (only) some sybodies show a clear preference for ATP-bound or unbound Smc, this is not a strong predictor of the strength of phenotype observed in vivo. We have also attempted to characterize the binding of Smc to sybodies by other methods including pull-downs, cross-linking, and by biophysical methods (GCI). However, we prefer to not include these data as the outcomes are not clear due to inconsistencies in the behaviour of purified sybodies.

> *(2) Many modes of sybody binding to Smc are plausible*
>
> *The authors provide an elaborate discussion of sybodies locking the Smc-ScpAB complex in open/ closed states. However, in the absence of structural support, the mechanistic*

> *inferences may need to be tempered. For example, is it also not possible for the sybodies to bind the inner interface of the coiled-coil, resulting in steric hinderance to coiled-coil interactions. It is also possible that sybody interaction disrupts ScpAB interaction (as data ruling this possibility out has not been provided). Thus, other potential mechanisms would be worth considering/ discussing. In this direction, did AlphaFold reveal any potential insights into putative binding locations?*

We have attempted to map the binding by structure prediction, however, so far, even the latest versions of AlphaFold are not able to clearly delineate the binding interface that we have confidently identified by the mapping using chimeric proteins. Indeed, many ways of binding are possible, including disruption of ScpAB interaction. However, since the mapped binding sites are located on the SMC coiled coils, the later scenario seems unlikely and would be an indirect consequence of altered coiled coil configuration, consistent with our current interpretation.

> *(3) Sybody expression in vivo*
>
> *Have the authors estimated sybody expression in vivo? Are they all expressed to similar levels?*

We have tagged selected sybodies with gfp and performed live cell imaging. This shows that sybodies without strong phenotypes are similarly expressed at least at low inducer concentration. Moreover, many sybodies localize as foci in the cell presumably by binding to Smc complexes loaded onto the chromosome at ParB/parS sites. We have included example data in the revised version of the manuscript as Figure S4 and Figure S5. Notably, a sybody (Sb007) with a weak growth phenotype shows focal localization at low inducer concentration and high expression levels when fully induced, comparable to sybodies with strong phenotypes. Altogether, this suggests that the lack of phenotype is not due to absence of sybody expression or localization.

> *(4) Sybodies should phenocopy ATP hydrolysis mutant of Smc*
>
> *The sybodies were screened against an ATP hydrolysis deficient mutant of Smc, with the rationale that these sybodies would interfere this step of the Smc duty cycle. Does the expression of the sybodies in vivo phenocopy the ATP hydrolysis deficient mutant of Smc? Could the authors consider any phenotypic read-outs that can indicate whether the sybody action results in an smc-null effect or specifically an ATP hydrolysis deficient effect?*

As alluded to above, we think that our selection gave rise to sybodies that bind various, possibly multiple Smc conformations. Consistent with this idea, the phenotypes of sybody expression are similar to null mutant rather than the ATP-hydrolysis defective EQ mutant, which display even more severe growth phenotypes in *B. subtilis*. To highlight this point, we have added the following notes to the text:

“These conditions favour ATP-engaged particles alongside the typically predominant ATP-disengaged rod-shaped state.”

“ELISA data revealed that nearly all clones bind purified Smc-ScpAB (Table 1). However, the ELISA signals of only few Sybodies showed clear dependence on the presence or absence of ATP and DNA (Table S1).”

> *Significance:*
>
> *Overall, this is an impressive study that uses an elegant strategy to find inhibitors of protein activity in vivo. The manuscript is clearly written and the experiments are logical and well-designed. The findings from the study will be significant to the broad field of*

genome biology, synthetic biology and also SMC biology. Specifically, the coiled coil domain of SMC proteins have been proposed to be of high functional value. The authors have elegantly identified key coiled-coil regions that may be important for function, and parallelly exhibited potential of the use of synthetic sybody/designed binders for inhibition of protein activity.

Reviewer #2 (Public review):

Summary:

Structural Maintenance of Chromosome proteins (SMCs), a family of proteins found in almost all organisms, are organizers of DNA. They accomplish this by a process known as loop extrusion, wherein double-stranded DNA is actively reeled in and extruded into loops. Although SMCs are known to have several DNA binding regions, the exact mechanism by which they facilitate loop extrusion is not understood but is believed to entail large conformational changes. There are currently several models for loop extrusion, including one wherein the coiled coil (CC) arms open, but there is a lack of insightful experimentation and analysis to confirm any of these models. The work presented aims to provide much-needed new tools to investigate these questions: conformation-selective sybodies (synthetic nanobodies) that are likely to alter the CC opening and closing reactions.

The authors produced, isolated, and expressed sybodies that specifically bound to Bacillus subtilis Smc-ScpAB. Using chimeric Smc constructs, where the coiled coils were partly replaced with the corresponding sequences from Streptococcus pneumoniae, the authors revealed that the isolated sybodies all targeted the same 4N CC element of the Smc arms. This region is likely disrupted by the sybodies either by stopping the arms from opening (correctly) or forcing them to stay open (enough). Disrupting these functional elements is suggested to cause the Smc-dependent chromosome organization lethal phenotype, implying that arm opening and closing is a key regulatory feature of bacterial Smc-ScpAB.

Significance:

The authors present a new method for trapping bacterial Smc's in certain conformations using synthetic antibodies. Using these antibodies, they have pinpointed the (previously suggested) 4N region of the coiled coils as an essential site for the opening and closing of the Smc coiled coil arms and that hindering these reactions blocks Smc-driven chromosomal organization. The work has important implications for how we might elucidate the mechanism of DNA loop extrusion by SMC complexes.

Reviewer #3 (Public review):

Summary:

Gosselin et al. use the sybody technology to study effects of in vivo inhibition of the Bacillus subtilis SMC complex. Smc proteins are central DNA binding elements of several complexes that are vital for chromosome dynamics in almost all organisms. Sybodies are selected from three different libraries of the single domain antibodies, using the "transition state" mutant Smc. They identify 14 such mutant sybodies that are lethal when expressed in vivo, because they prevent proper function of Smc. The authors present evidence suggesting that all obtained sybodies bind to a coiled-coil region close to the Smc "neck", and thereby interfere with the Smc activity cycle, as evidenced by defective ATPase activity when Smc is bound to DNA.

The study is well done and presented and shows that the strategy is very potent in finding a means to quickly turn off a protein's function in vivo, much quicker than depleting the

> *protein.*
>
> *The authors also draw conclusions on the molecular mode of action of the SMC complex. The provide a number of suggestive experiments, but in my view mostly indirect evidence for such mechanism.*
>
> *My main criticism is that the authors have used a single - and catalytically trapped form of SMC. They speculate why they only obtain sybodies from one library, and then only identify sybodies that bind to a rather small part of the large Smc protein. While the approach is definitely valuable, it is biassed towards sybodies that bind to Smc in a quite special way, it seems. Using wild type Smc would be interesting, to make more robust statements about the action of sybodies potentially binding to different parts of Smc.*

The reviewer reports (Rev. #1 and Rev. #3) made us realize that the manuscript text was misleading on the this point. Although we used the purified ATP hydrolysis–deficient Smc protein for sybody isolation, this is not expected to restrict the selection to a specific conformation. As described in detail in Vazquez-Nunez et al. (Figure 5), this mutant displays the ATP-engaged conformation only in a smaller fraction of complexes (~25% in the presence of ATP and DNA), consistent with prior in vivo observations reported by Diebold-Durand et al. (Figure 5). Rather than limiting the selection to a particular configuration, our aim was to reduce the prevalence of the predominant rod state in order to broaden the range of conformations represented during sybody selection. Consistent with this interpretation, only a small number of isolated sybodies show strong conformation-specific binding in the presence or absence of ATP/DNA, as observed by ELISA (now included in the manuscript). Notably, the effect size of ATP/DNA on ELISA signals was not a strong predictor to the strength of phenotypes observed in vivo. The text has been revised accordingly. See line 84 and line 92.

We are thus quite confident based prior work (and on the now included ELISA data) that the Smc ATPase mutation did not strongly bias the selection in one way or another. The surprising bias towards coiled coil binding sites has likely other explanations, as they likely form a preferred epitope recognized by sybodies from the loop library.

> *Line 105: Alternatively, the other libraries did not produce good binders or these sybodies were 106 not stably expressed in B. subtilis. This could be tested using Western blotting - I am assuming sybody antibodies are commercially available. However, this test is not important for the overall study, it would just clarify a minor point.*

While there are antibody fragments available to augment the size of sybodies (PMID: 40108246), these recognize 3D-epitopes and are thus not suited for Western blotting. We did not follow up on the negative results of two of the three libraries but would like to point out again that there are several biases that likely emerge for the same reason (bias to library, bias to coiled coil binding site). If correct, then sybodies are likely ineffective in inactivating Smc in B. subtilis, with the notable exceptions of the sybodies that we have isolated and characterized in this manuscript. We have added this notion to the manuscript.

> *Fig. 2B: is odd to count Spo0J foci per cells, as it is clear from the images that several origins must be present within the fluorescent foci. I am fine with the "counting" method, as the images show there is a clear segregation defect when sybodies are expressed, I believe the authors should state, though, that this is not a replication block, but failure to segregate origins.*

We agree that this is an important point. We have added the following statement to clarify this point: “These elongated cells are known to harbour expanded nucleoids, consistent with delayed oriC separation rather than delayed DNA replication”

> *Testing binding sites of sybodies to the SMC complex is done in an indirect manner, by using chimeric Smc constructs. I am surprised why the authors have not used in vitro*

> *crosslinking: the authors can purify Smc, and mass spectrometry analyses would identify sites where sybodies are crosslinked to Smc. Again, I am fine with the indirect method, but the authors make quite concrete statements on binding based on non-inhibition of chimeric Smc; I can see alternative explanations why a chimera may not be targeted.*

We have made several attempts of testing direct binding with mixed outcomes and decided to not include those results in the light of the stronger and more relevant in vivo mapping. However, we have added ELISA results (new Table S1) that support a direct interaction.

> *Smc-disrupting sybodies affect the ATPase activity in one of two ways. Again, rather indirect experiments. This leads to the point Revealing Smc arm dynamics through synthetic binders in the discussion. The authors are quite careful in stating that their experiments are suggestive for a certain mode of action of Smc, which is warranted.*
>
> *In line 245, they state More broadly, the study demonstrates how synthetic binders can trap, stabilize, or block transient conformations of active chromatin-associated machines, providing a powerful means to probe their mechanisms in living cells. This is off course a possible scenario for the use of sybodies, but the study does not really trap Smc in a transient conformation, at least this is not clearly shown.*

We agree and have simplified the statement by removing “stabilize” and “transient”.

> *Overall, it is an interesting study, with a well-presented novel technology, and a limited gain of knowledge on SMC proteins.*

We respectfully disagree with the last point, since our unique results highlight the importance of the Smc coiled coils. which are less well represented in the SMC literature (when compared to the heads and hinge domains for example), likely (at least in part) due the mild effect of single point mutations on coiled coil dynamics.

> *Significance:*
>
> *The work describes the gaining and use of single-binder antibodies (sybodies) to interfere with the function of proteins in bacteria. Using this technology for the SMC complex, the authors demonstrate that they can obtain a significant of binders that target a defined region is SMC and thereby interfere with the ATPase cycle.*
>
> *The study does not present a strong gain of knowledge of the mode of action of the SMC complex.*

As pointed out above, we respectfully disagree with this assertion.

https://doi.org/10.7554/eLife.111131.2.sa0